

1 **Rapid climatic changes and resilient vegetation during the Lateglacial and**
2 **Holocene in a continental region of south-western Europe**

3 Josu Aranbarri (1, 2, 3*), Penélope González-Sampériz (1), Blas Valero-Garcés (1),
4 Ana Moreno (1), Graciela Gil-Romera (1), Miguel Sevilla-Callejo (1), Eduardo García-
5 Prieto (1); Federico Di Rita (2), M. Pilar Mata (4), Mario Morellón (5), Donatella Magri
6 (2), Julio Rodríguez-Lázaro (3), José S. Carrión (6)

7 (1) Instituto Pirenaico de Ecología-CSIC Avda. Montañana 1005, 50059 Zaragoza,
8 Spain

9 josu.aran@ipe.csic.es; pgonzal@ipe.csic.es; blas@ipe.csic.es; amoreno@ipe.csic.es;
10 graciela.gil@ipe.csic.es; msevilla@ipe.csic.es; eduardogpf@ipe.csic.es

11 (2) Dipartimento di Biologia Ambientale, Sapienza Università di Roma, Piazzale Aldo
12 Moro, 5, 00185 Rome, Italy josu.aranbarri@uniroma1.it; federico.dirita@uniroma1.it;
13 donatella.magri@uniroma1.it

14 (3) Departamento de Estratigrafía y Paleontología, Universidad del País Vasco-Euskal
15 Herriko Unibertsitatea, B. Sarriena s/n, Ap. 644, 48080 Bilbao, Spain
16 julio.rodriguez@ehu.es

17 (4) Instituto Geológico y Minero de España, C. La Calera, 1, 28760 Tres Cantos, Spain
18 p.mata@igme.es

19 (5) Instituto de Geociencias-CSIC, UCM, Universidad Complutense de Madrid, C. José
20 Antonio Nováis, 2, 28040, Madrid, Spain mario.morellon@igeo.ucm-csic.es

21 (6) Departamento de Biología Vegetal, Universidad de Murcia, 30100 Murcia, Spain
22 carrion@um.es

23 * Author for correspondence: josu.aran@ipe.csic.es

26 **Abstract**

27 Palynological, sedimentological and geochemical analyses performed on the
28 Villarquemado paleolake sequence (987 m a.s.l, 40°30'N; 1°18'W) reveal the vegetation
29 dynamics and climate variability in continental Iberia over the last 13500 cal yr BP. The
30 Lateglacial and early Holocene periods are characterized by arid conditions with a
31 stable landscape dominated by pinewoods and steppe until ca. 7780 cal yr BP, despite
32 sedimentological evidence for large paleohydrological fluctuations in the paleolake. The
33 most humid phase occurred between ca. 7780-5000 cal yr BP and was characterized by
34 the maximum spread of mesophytes (e.g., *Betula*, *Corylus*, *Quercus faginea* type), the
35 expansion of a mixed Mediterranean oak woodland with evergreen *Quercus* as
36 dominant forest communities and more frequent higher lake level periods. The return of
37 a dense pinewood synchronous with the depletion of mesophytes characterizes the mid-
38 late Holocene transition (ca. 5000 cal yr BP) most likely as a consequence of an
39 increasing aridity that coincides with the reappearance of a shallow, carbonate wetland
40 environment. The paleohydrological and vegetation evolution shows similarities with
41 other continental Mediterranean areas of Iberia and demonstrates a marked resilience of
42 terrestrial vegetation and gradual responses to millennial-scale climate fluctuations.
43 Human impact is negligible until the Ibero-Roman period (ca. 2500 cal yr BP) when a
44 major deforestation occurred in the nearby pine forest. The last 1500 years are
45 characterized by increasing landscape management, mainly associated with grazing
46 practices shaping the current landscape.

47

48 **Key words:** Holocene, Multiproxy reconstruction, Vegetation resilience, Pinewoods,
49 Aridity, Continental Iberia

50

51 **1. Introduction**

52 The progressive increase in the number of well-dated, high-resolution Holocene climate
53 records in both marine and continental areas (Hoek et al., 2008; Lowe et al., 2008) has
54 demonstrated the existence of complex millennial-scale oscillations and rapid climate
55 changes in response to both extraterrestrial forcings (e.g., orbital parameters, insolation,
56 etc.) and internal mechanisms (e.g., changes in deep-ocean circulation, internal climate
57 system variability) (Bond et al., 1997; Alley et al., 2003; Mayewski et al., 2004; Denton
58 and Broecker, 2008; Wanner et al., 2008; Renssen et al., 2009). In particular, the
59 western Mediterranean Basin, strategically located under the incursion of North-Atlantic
60 storm tracks and the influence of a high pressure system in summer-months, is a
61 fundamental region to understand the climate evolution and the vegetation response to
62 abrupt changes and perturbations originated at high (Fletcher and Sánchez Goñi, 2008)
63 and lower latitudes (Peyron et al., 2011). Indeed, several marine cores from the western
64 Iberian margin demonstrate the impact of short-lived Holocene climatic events (e.g.,
65 Preboreal Oscillation, 8200 cal yr BP event, 4200 cal yr BP aridity crisis) on vegetation
66 firstly identified in North Atlantic cores (Alley et al., 1997; Björck et al., 1997;
67 Rasmussen et al., 2007) and then recorded in the Iberian Peninsula as dry spells and
68 probably cool conditions (Cacho et al., 2001; Frigola et al., 2007; Combourieu Nebout
69 et al., 2009; Fletcher et al., 2010). Iberian sedimentary sequences have reported similar
70 Holocene oscillations, clearly documented by prominent peaks of xerophytes in pollen
71 records (Muñoz Sobrino et al., 2005; González-Sampériz et al., 2006; Fletcher et al.,
72 2007; Moreno et al., 2011; Pérez-Sánchez et al., 2013), by abrupt drops in lake water-levels
73 (Carrion, 2002; González-Sampériz et al., 2008; Martín-Puertas et al., 2008; Morellón
74 et al., 2009), and complex patterns of human adaptations (González-Sampériz et al.,
75 2009; Cortés-Sánchez et al., 2012).

76 Regarding ecosystem responses to climate change, recent reviews have highlighted the
77 unidirectional response of the Iberian phytodiversity throughout the late Quaternary
78 (Carrión et al., 2010a; González-Sampériz et al., 2010), where regional ecological
79 dissimilarities, enhanced by particular orographic and edaphic features, have prevented
80 the unraveling of common climatic patterns. Ecosystem inertia to Lateglacial and
81 Holocene climate changes has been a clear example of the mentioned unidirectional
82 trend (e.g., Carrión and van Geel, 1999; Franco-Múgica et al., 2001, 2005; García-
83 Antón et al. 2011; Morales-Molino et al., 2012), being long-term pinewood resilience
84 the main distinctive aspect of wide areas of continental Iberia (Rubiales et al., 2010, and
85 references therein).

86 Despite the number of Lateglacial and Holocene palaeoenvironmental sequences in the
87 Iberian Peninsula increased during the last decades (Carrión et al., 2010a and references
88 therein), the continental lowlands of Iberia have hardly been investigated, leaving a
89 palaeobiogeographical gap between inner continental mountains and coastal areas.
90 Climatically located near the Ebro Basin, the Iberian Range borders the northernmost
91 area of truly semi-arid climate in Europe, whose patchy and fragile steppe-like
92 vegetation is strongly conditioned by an arid climate regime and edaphic constraints
93 (Vicente-Serrano et al., 2012; Pueyo et al., 2013). Permanent lakes are absent in the
94 region and therefore, most of the regional paleorecords have been obtained from large
95 ephemeral or hypersaline lakes (Valero-Garcés et al., 2000a,b, 2004; Davis and
96 Stevenson. 2007; Luzón et al., 2007; González-Sampériz et al., 2008; Sancho et al.,
97 2011; Gutiérrez et al., 2013), where recurrent hiatuses and complex geochemical
98 processes often hamper chronological control and pollen preservation, preventing
99 continuous high-resolution environmental reconstructions (González-Sampériz et al.,
100 2008). Further southwest from the Ebro Basin, studies providing detailed climatic

101 oscillations are available. These are derived mainly from lake level fluctuations and
102 paleoflood frequency records, although they cover relatively short timescales spanning
103 only the last three millennia (Moreno et al., 2008; Romero-Viana et al., 2011; López-
104 Blanco et al., 2012; Barreiro-Lostres et al., 2013). Additional paleoenvironmental
105 information, somewhat fragmentary and influenced by local peculiarities, is provided by
106 geomorphological (Valero-Garcés et al., 2008; Constante et al., 2011) and
107 archaeological studies (González-Sampéris et al., 2009; Aura et al., 2011; Utrilla et al.,
108 2012).

109 Based on a multiproxy approach, the well-dated and continuous sedimentary sequence
110 obtained from the Villarquemado paleolake offers the possibility to reconstruct the
111 postglacial palaeoenvironmental history of a poorly-studied, ecotonal and continental,
112 Mediterranean area. The main goals of the current study are to:

- 113 1) Understand both regional and local vegetation dynamics and hydrological response to
114 the last ca. 13500 cal yr BP climate variability.
- 115 2) Place the Villarquemado vegetation development in regional context through
116 correlation with other well-dated pollen records.
- 117 3) Explore the sensitivity of this and other ecotonal regions to detect Holocene abrupt
118 climate changes, especially in areas where pinewoods have been the dominant
119 communities.

120 **2. Regional Setting**

121 Villarquemado paleolake (40°30'N; 1°18'W, **Figure 1**) is located at about 1000 m a.s.l.,
122 in the Jiloca Basin (Iberian Range, NE Spain). This is a 60 km long, 6-10 km wide, N-S
123 half-graben, bounded by NW-SE trending normal faults. The depression belongs to a
124 series of intramontane basins developed in the Iberian Range during the second
125 extensional episode that started in the Upper Pliocene (Simón-Gómez, 1989; Casas-

126 | [Sainz and De Vicente, 2009](#)). The change from endorheic to exorheic conditions in
127 these depressions occurred during the Neogene and Plio-Quaternary through the capture
128 of the basins by the external drainage network and headwater erosion ([Gutiérrez and](#)
129 [Gracia, 1997](#)). The Jiloca river captured the Daroca half-graben and subsequently the
130 next depression to the south, the Jiloca Depression ([Gracia et al., 2003](#)). However the
131 south-central sector of this depression remained an endorheic basin until it was
132 artificially drained in the 18th century, when the maximum flooded area was 11.3 km²
133 and the water depth up to 2.8 m ([Rubio, 2004](#)).

134 The current climate of the region is continental Mediterranean, characterized by severe
135 summer droughts, strong seasonal and diurnal temperature oscillations and by relatively
136 low precipitation values ([Figure 2B](#)). The maximum absolute temperature is about 40 °C
137 in summer and the winter minimum can reach -15 °C with frequent freezing days in the
138 region. The mean annual precipitation in the area is about 380 mm ([Figure 2B](#): Cella
139 station, 1023 m a.s.l.), with large interannual variability and irregular distribution
140 through the year, while higher elevations are influenced by more regular orographic
141 precipitations ([Figure 2C](#): Griegos station, 1604 m a.s.l.). Regional-scale rainfall
142 dynamics is principally controlled by the westerly winds, associated with cold fronts in
143 spring and high-intensity convective storms in autumn. During the summer, the
144 subtropical Azores anticyclone blocks the moisture from the west and brings warm and
145 dry air masses from the south, being the negative water balance associated to high
146 evapotranspiration values ([Figure 2C](#)).

147 The Villarquemado paleolake is located in the mesomediterranean bioclimatic belt, with
148 *Quercus ilex* and *Quercus faginea* as principal tree species, along with other
149 Mediterranean xerophytic shrubs (*Rhamnus alaternus*, *Genista scorpius*, *Ephedra*
150 *fragilis*, *Thymus* spp.) and herbs (*Artemisia assoana*, *A .campestris*, *Atriplex prostrata*,

151 *Salicornia ramosissima* (Figure 2D). The calcareous soils in the area support *Juniperus*
152 *phoenicea* and *J. thurifera*. The supramediterranean belt is characterized by *Pinus*
153 *sylvestris* communities with *Buxus sempervirens* and *Juniperus sabina*. In red
154 sandstones areas, *Pinus pinaster* woodlands, with dense Cistaceae and Ericaceae shrubs,
155 prevail. The hydroseral community is dense, well developed and linked to seasonal
156 water level fluctuations. The dominant species here are *Phragmites australis*, *Juncus*
157 *acutus*, *J. inflexus*, *J. maritimus* and *Scirpus holoschoenus*; scattered trees of *Salix*
158 *fragilis* and *S. atrocinerea* with a scrubland of *Crataegus monogyna* and some *Populus*
159 *canadensis* cultivars. The natural wetland vegetation has been substantially modified by
160 agriculture and grazing (Figure 2D).

161 **3. Material and methods**

162 A 74 m long sediment core (core VIL-05-1B) was retrieved in 2005 from the deepest
163 area of the Villarquemado wetland, using a truck-mounted drilling system (Moreno et
164 al., 2012a; González-Sampérez et al., 2013). The extracted material was extruded,
165 transported to IPE-CSIC laboratory and stored at 4°C until required for analysis. The top
166 61 cm were disturbed due to the coring system and were not considered for analysis. To
167 complete the 0-61 cm gap, a parallel 247 cm long core (core VIL-05-1A) was taken
168 with a modified 5 cm-diameter Livingstone piston corer, a coring system that allows
169 recovering unaltered the uppermost part of the sequence.

170 Correlation between cores VIL-05-1A and VIL-05-1B was achieved using sedimentary
171 facies, radiocarbon dating and pollen stratigraphy (Figure 3A). Therefore, the composite
172 sequence of the Villarquemado paleolake was built using the uppermost 40 cm of the
173 shorter core VIL-05-1A and the core VIL-05-1B, excluding the first 61cm (Figure 3B).

174 The cores were longitudinally opened and the sedimentary facies described according to
175 Schnurrenberger et al. (2003). Geochemical data were obtained at 0.5 cm intervals by

176 means of an XRF ITRAX Core scanner at the Large Lakes Observatory (University of
177 Minnesota, USA). Total inorganic carbon (TIC) was analyzed every 2 cm with a LECO
178 SC 144 DR elemental analyzer at the IPE-CSIC laboratory, after the organic matter had
179 been removed. In addition, selected samples were analyzed by X-ray diffraction with a
180 Philips PW1820 diffractometer and relative mineral abundance was determined using
181 peak intensity to characterize the sedimentological facies. All the geochemical and
182 elementary analyses were performed exclusively in core VIL-05-1B.

183 Samples for pollen analysis were taken every 2-3 cm intervals in the core VIL-05-1B
184 while in the core VIL-05-1A only 15 samples were retrieved to complete the uppermost
185 part of the sequence. Pollen extraction followed the standard chemical procedure
186 (Moore et al., 1991).

187 Pollen identification was supported by the reference collection from IPE-CSIC,
188 determination keys and photo atlases (Reille, 1992). Results are expressed as
189 percentages, excluding hygrophytes, hydrophytes, Pteridophyta spores and other non
190 pollen palynomorphs (NPP) from the pollen sum. The Psimpoll 4.27 software (Bennett,
191 2009) was used to draw the pollen diagram. Major palynological changes in pollen
192 composition as well as cluster analysis, CONISS (Grimm, 1987), were used as criteria
193 to subdivide the results into pollen assemblage zones.

194 The chronology of the core VIL-05-1B was established on the basis of five AMS ^{14}C
195 dates, obtained from bulk sediment samples. In addition, other three AMS ^{14}C dates
196 were retrieved from core VIL-05-1A. ^{14}C data were calibrated using Calib 6.11 (Stuiver
197 and Reimer, 1993) with IntCal09 calibration datasets (Reimer et al., 2009) (Table 1) and
198 the composite age-depth model (lineal interpolation) was obtained using the *Clam*
199 software package for age-depth modeling (Blaauw, 2010) (Figure 3B). The

200 chronological model shows a fairly constant accumulation rate, ca. 0.049 cm yr⁻¹, which
201 spans from ca. 13500 to ca. 470 cal yr BP (Figure 3B).

202 4. Results

203 4.1. The sedimentological sequence

204 Visual description, smear slides microscopic observation, geochemical and
205 mineralogical analyses allowed seven main sedimentary facies to be determined in
206 Villarquemado paleolake sequence, later organized in three well-defined
207 sedimentological units (Figure 4).

208 The base of the sequence corresponds to **UNIT-3** (311-233 cm depth, 13540-11240 cal
209 yr BP), which is composed of medium, massive light grey carbonate silts (*facies 1*)
210 grading upwards to coarser, dark grey carbonate silts (*facies 2*). *Facies 1* and 2 are
211 characterized by relatively high siliciclastic content, as shown by mineral composition
212 (significant quartz content) and by the maximum values of Si, Ti and Fe (Figure 4). In
213 particular, silicates (quartz and feldspars) in *facies 2* range between 25-50 % versus 50-
214 75% calcite. Subunit **SUB-3B** (311-256 cm, 13540-12170 cal yr BP), is relatively more
215 carbonate-rich, with TIC (total inorganic carbon) up to 6%, and subunit **SUB-3A** (256-
216 233 cm, 12170-11240 cal yr BP) has the highest silicate content of the whole sequence
217 (only 3% TIC). The top of UNIT-3 is a sharp depositional surface in both
218 Villarquemado cores (VIL-05-1A and VIL-05-1B) and it is located at approximately the
219 same depth (ca. 230 cm). This transition from siliciclastic-rich to carbonate-rich
220 sediments at the boundary between UNIT-3 and 2 is used as a correlation horizon (tie-
221 point 1, TP-1) (Figure 3A).

222 **UNIT-2** (233-61 cm depth, 11240-1940 cal yr BP) is an alternation of fine to medium,
223 banded, creamy carbonate silts organized in dm-thick intervals (*facies 3*) and dark grey,
224 mottled, massive, carbonate and organic-rich silts as cm-thick layers (*facies 4*). *Facies 3*

225 is made of endogenic carbonates precipitated in the palustrine and littoral lake
226 subenvironments (e.g., Charophyceae, carbonate coatings) with maximum Ca values.
227 *Facies 4* has about 5% silicate content (clay minerals and quartz) marked by slight
228 increases in the chemical elements associated to the siliciclastic fraction (Si, Fe, Ti).
229 Both facies contain mm to cm-sized plant remains, suggesting a shallow depositional
230 environment (littoral area). Mottled and soil textures (roots, bioturbation) are especially
231 abundant in the grey silts indicating more frequent subaerial exposition.

232 UNIT-2 has been divided into three subunits depending on sedimentary facies and
233 geochemical composition: SUB-2C (233-192 cm) is composed by *facies 3* creamy
234 carbonate silts. SUB-2B (192-140 cm) is characterized by the predominance of *facies 4*
235 with intercalations of more organic-rich facies (*facies 6*) and cm-thick coarse silt-fine
236 sand carbonate-rich layers (*facies 5*). The presence of these organic-rich sediments in
237 both sediment cores represents another correlation marker (TP-3) (Figure 3A). Finally
238 SUB-2A (140-61 cm) represents the association of *facies 3* and *4*, with relatively higher
239 carbonate content.

240 **UNIT-1** (61-0 cm depth, post 1940 cal yr BP) is composed of dark brown to dark grey,
241 massive, coarse peaty silt, with abundant plant fragments (*facies 7*) in VIL-05-1B and
242 *facies 4* with two cm-thick intercalations of *facies 3* in core VIL-05-1A. UNIT-1 is
243 composed of unconsolidated material; therefore geochemical properties were not
244 analysed. As a result, correlation between the uppermost sections of the two cores (VIL-
245 05-1A and VIL-05-1B) (TP-4) is based on the pollen composition (Figure 3A), as
246 explained below.

247 **4.2. The pollen sequence**

248 The preservation of pollen grains was generally good. Composite pollen diagrams are
249 presented in the **Figures 5 and 6** showing the analytic results of 99 samples. Six
250 Villarquemado pollen assemblage zones (VIL) have been established.

251 **VIL-6 (311-233 cm depth; ca. 13540-11240 cal yr BP), Sedimentary UNIT-3**

252 Based on the variation of Cyperaceae, *Typha/Sparganium* type, hydrophyte-group and
253 Pteridophytes, two subzones have been defined:

254 **VIL-6B** (311-256 cm depth; ca. 13540-12170 cal yr BP) is characterized by relatively
255 low, fluctuating arboreal pollen (AP). *Pinus nigra/sylvestris* type is dominant (**Figure**
256 **5**). Other trees are less important, such as *Juniperus* amongst the conifers; both *Quercus*
257 *faginea* type and evergreen *Quercus* are rare, as well as *Betula*, *Salix*, *Ulmus* and
258 *Fraxinus*. Shrubs such as *Tamarix*, *Ephedra fragilis* and *Ephedra distachya* type show
259 minor occurrences. Xerophytes are well represented, with *Artemisia*, Chenopodiaceae
260 and Compositae as main contributors (**Figures 6**). Poaceae is relatively abundant and
261 within the hygrophytic community, Cyperaceae show the highest percentages of the
262 sequence, accompanied by high frequencies of *Ranunculus*, Juncaceae,
263 *Typha/Sparganium* type and a significant presence of *Myriophyllum* and *Potamogeton*.

264 **VIL-6A** (256-233 cm depth; ca. 12170-11240 cal yr BP) is defined by a drastic change
265 in the hygrophyte community (**Figure 6**). Particularly, the transition from sedimentary
266 subunit SUB-3B to SUB-3A corresponds to the replacement of the previous
267 Cyperaceae-dominated environment (with abundant Juncaceae and *Ranunculus*) with a
268 *Typha/Sparganium* type community. This hydrological change is also marked by the
269 highest development of submerged aquatic plants (*Myriophyllum* and *Potamogeton*) and
270 the maximum frequencies of Pteridophyta spores (**Figure 6**).

271 **VIL-5 (233-164 cm depth; ca. 11240-7780 cal yr BP), Sedimentary UNIT-2; SUB-**
272 **2C, SUB-2B**

273 Oscillations in AP frequencies allow two subzones to be defined:
274 During the **VIL-5B** (233-192 cm depth; ca. 11240-9140 cal yr BP) xerophytes, mainly
275 *Artemisia* and Chenopodiaceae, rise considerably (Figure 6). AP values are still low.
276 *Pinus nigra/sylvestris* type frequencies decrease, although *Juniperus* increases
277 significantly (Figure 5). Broadleaved trees like *Betula*, and both *Quercus* types are
278 recorded. *Tamarix* development is noticeable.

279 **VIL-5A** (192-162 cm depth; ca. 9140-7780 cal yr BP) is defined by progressive
280 increases of *Betula*, *Corylus*, and both *Quercus* (Figure 5). A progressive coeval
281 decrease in *Artemisia*, Chenopodiaceae, hygrophytes and hydrophytes is noticed (Figure
282 6).

283 **VIL-4 (164-112 cm depth; ca. 7780-5000 cal yr BP), Sedimentary UNIT-2; SUB-**
284 **2B, SUB-2A**

285 This zone is characterized by the maximum abundance of deciduous trees (*Corylus*,
286 *Quercus faginea* type, *Alnus*, *Salix*, *Ulmus*, *Fraxinus*, *Fagus* and *Tilia*), a decline of the
287 *Pinus nigra/sylvestris* type frequencies, and a decrease in xerophyte values. This is
288 synchronous with an increase in thermophilous elements; evergreen *Quercus* is the most
289 important arboreal element and its expansion parallels the maximum frequencies of
290 Mediterranean shrubs (*Pistacia*, *Rhamnus*, *Phillyrea*, *Buxus*, *Thymelaea*) and the
291 continuous presence of Ericaceae, Rosaceae, Fabaceae and Lamiaceae (Figures 5 and
292 6). Continuous values of *Juniperus* and a significant presence of *Artemisia* are recorded.
293 Poaceae diminishes significantly, while the hygro-hydrophytic component falls to its
294 sequence minimum (Figure 6).

295 **VIL-3 (112-71 cm depth; ca. 5000-2530 cal yr BP), Sedimentary UNIT-2; SUB-2A**

296 During VIL-3, both *Pinus nigra/sylvestris* type and *Pinus pinaster/hapensis* type show
297 important increases. Overall, mesophytes are decreasing, which affects especially to

298 *Corylus*, while *Betula* and *Tilia* disappears. This zone also shows fluctuating evergreen
299 *Quercus*. Although scant along previous zones, *Olea* occurs continuously showing a
300 gradual increasing trend (Figure 5). During this period, pollen grains of *Cedrus* are
301 recorded at 116, 103 and 99 cm depth (ca. 5230, 4490 and 4260 cal yr BP respectively).
302 Hygrophyte and hydrophyte pollen grains occur in low abundances, similarly to the
303 previous zone (Figure 6).

304 **VIL-2 (71-62 cm depth; ca. 2530-1940 cal yr BP), Sedimentary UNIT-2; SUB-2A**

305 A major change in forest structure is the main feature of this zone. *Pinus* reaches a
306 minimum, and *Quercus faginea* and evergreen *Quercus* show significant expansions
307 (Figure 5 and 6).

308 **VIL-1 (61-32 cm depth; ca. 1940-470 cal yr BP), Sedimentary UNIT-1**

309 *Pinus nigra/sylvestris* type values partially rise while both *Quercus faginea* type and
310 evergreen *Quercus* decline. AP is low (Figure 5) while the herb component
311 (Compositae, Chenopodiaceae, *Artemisia*, Lamiaceae and Fabaceae) exhibits a large
312 increase. Coprophilous fungal spores, dominated by Sordariales peak while a maximum
313 in *Glomus* chlamydospores is seen (Figure 6).

314 **5. Discussion**

315 **5.1. Climate, vegetation and hydrological variability during the last 13500 cal yr BP**

316 **5.1.1. The Last Glacial-Interglacial transition (LGIT): resilient vegetation and**
317 **hydrological variability (13540-11270 cal yr BP)**

318 Last Glacial-Interglacial transition (LGIT) at Villarquemado was characterized by
319 deposition of sediments with high siliciclastic content compared with the Holocene
320 interval (Figure 4). The vegetation cover was composed by a relatively high amount of
321 xerophytes (Figures 5 and 6) and the dominance of *Pinus nigra/sylvestris* type among
322 the AP, with values around 40%. These percentages suggest the presence of some tree

323 patches in an open landscape around the lake or a montane pinewood at higher altitudes,
324 similarly to the present-day situation. Deciduous elements were poorly represented and
325 probably were confined to riverbanks (e.g., *Ulmus*, *Salix*, *Fraxinus*) or in particular
326 humid shelters of the Albarracín Range (Figure 5). The lack of a mesophyte vegetation
327 expansion in response to the Allerød interstadial (GI-1a) period (Björck et al., 1997),
328 corresponding to VIL-6B pollen zone according to our chronological model, differs
329 from other Iberian areas where a broadleaf forest expansion has been recognized (Pons
330 and Reille, 1988; Peñalba, 1994; Pérez-Obiol and Julià, 1994; Gil-García et al. 2002;
331 González-Sampériz et al. 2006; Muñoz Sobrino et al., 2013). The lagged vegetation
332 response to the GI-1a climate signal is attributable to the resilience of the continental
333 ecosystems to increased moisture availability, although vegetation dynamics may be
334 partly masked by the low sample resolution of this interval (Figures 7 and 8). The
335 resilient behaviour of the vegetation continues during the Younger Dryas (GS-1)
336 chronozone (Björck et al., 1997) when no major changes in the forest physiognomy are
337 recorded (Figures 5 and 8). Nevertheless, the increase in *Pinus* between 13200 and
338 12200 cal yr BP (VIL-6B) may partially reflect an altitudinal migration of the of the
339 pinewood treeline associated with the onset of cooler conditions at higher elevations.
340 Unfortunately, this hypothesis cannot be tested through correlation due to the lack of
341 Lateglacial paleoecological records at higher altitudes in our study area. In addition, the
342 Younger Dryas is not always clearly documented in the eastern Iberian sequences
343 (Carrión et al., 2010a and references therein), suggesting a low impact of this event in
344 pine woodlands.

345 Therefore, although no important changes in the regional vegetation during the LGIT
346 are clearly recorded, local aquatic taxa and sedimentological indicators point to
347 relatively high water levels and sediment delivery. In fact, hydrophytes reach their

348 maximum values during this period, especially in the VIL-6A interval (12170-11230 cal
349 yr BP), showing a remarkable shift from Cyperaceae-rich to a Typha-rich ecosystem
350 with large amounts of *Myriophyllum* and *Potamogeton* (Figures 6 and 8). These
351 coincide with the high proportions of Ti and the siliciclastic composition of UNIT-3,
352 particularly in SUB-3A, which indicate a lacustrine environment dominated by detrital
353 supply to the basin (Figure 4). Such a situation would be related to an increase in the
354 creeks/local rivers activity in the catchment as a response of (1) more intense rainfall
355 events and/or (2) colder conditions in an open landscape. Both situations would favor
356 erosion and the accumulation of detrital particles in the lake. The synchronous increase
357 in aquatic pollen during the LGIT, indicating higher lake level, supports this hypothesis.
358 The high lake level postulated for GS-1 would probably benefit from the decrease of
359 evaporation rates as a consequence of the reduced annual temperatures in a global-scale
360 cold period (Cacho et al., 2001; Moreno et al., 2010; Shakun and Carlson, 2010).

361 ***5.1.2. The early Holocene: vegetation and hydrological response to marked***
362 ***seasonality (11270-7780 cal yr BP)***

363 The early phase of the Holocene in the region was still dominated by a steppe landscape
364 (VIL-5B), although a progressive development of more water-demanding temperate
365 taxa (e.g., *Betula*, *Corylus* and *Quercus faginea* type) occurred from ca. 9140 cal yr BP
366 (VIL-5A), suggesting increased temperature and humidity (Figure 5). In agreement with
367 other Mediterranean sequences from the north-eastern sector of the Iberian Peninsula,
368 inner continental regions like the Villarquemado paleolake area were characterized by
369 the prevalence of cool and arid conditions at the beginning of the Holocene (e.g., Lake
370 Estanya, Morellón et al., 2009; Vegas-Vilarrúbia et al., 2013) with a remarkable
371 persistence of Lateglacial xeric communities and pinewoods in the vegetation cover
372 (González-Sampériz et al., 2005, and references therein). In particular, at Las Pardillas

373 Lake (Figure 1), steppe-like vegetation composed by *Juniperus*, *Artemisia* and Poaceae
374 was well represented prior to ca. 10500 cal yr BP (Sánchez Goñi and Hannon, 1999)
375 while at the nearby Ojos del Tamedal, situated in the Albarracín Range (Figure 1), a
376 treeless environment persisted until ca. 9600 cal yr BP (Stevenson, 2000). The limited
377 spread of mesic and thermophilous vegetation in Fuentillejo Maar (Vegas et al., 2010),
378 inner continental Iberia (Figure 1), was also associated with a dry and probably cold
379 climate regime during the first stages of the Holocene.

380 In southern and south-eastern Iberian intra-montane valleys and mid-altitude elevations,
381 the same environmental conditions of the inner continental areas are clearly visible
382 during this period. Thus, Navarrés (Carrión and van Geel, 1999), Villaverde (Carrión et
383 al., 2001) and Siles (Carrión, 2002) exhibit a similar pattern of conifer prevalence
384 during the first millennium of the Holocene as these communities are highly resilient
385 and their fluctuations present a more inertial character (Figure 7). In a recent review,
386 Rubiales et al. (2010) proposed that pinewoods spread in the Iberian mountains since
387 the LGM until ca. 8000 yr BP, suggesting that empty ecological niches available after
388 full-glacial climate conditions may have favoured the early colonization of *Pinus* in a
389 still dry climatic scenario. Consequently, not only during Lateglacial times but also
390 during the early Holocene, pinewoods would have been better adapted, climatically
391 favoured and easily dispersed from multiple stands with respect to broadleaved species
392 in medium altitude continental areas. Our data are coherent with the hypothesis by
393 Rubiales et al. (2010) which points to a regional dominance of *Pinus* until 7780 cal yr
394 BP in the lowlands of the Albarracín Range (Figures 5 and 7).

395 Model simulations for Eurasia confirmed that increased summertime insolation in the
396 Northern Hemisphere at the Holocene onset caused an increase in summer temperatures
397 (Rimbu et al., 2003; Kim et al., 2004). Paleocological data in central and northern

398 Europe have showed an almost immediate response of terrestrial ecosystems to the rise
399 in temperature during the early Holocene, visible by major fluctuations in the alpine
400 timberline (Ali et al., 2003; Tinner and Kaltenrieder, 2005) and by the expansion of
401 broadleaved trees reaching northern areas, even above the modern distributional range
402 limit (Kullman, 2013, and references therein). Reduced winter insolation also implied
403 minimum winter temperatures and extreme continentality due to the maximum
404 amplitude of solar forcing. Thus, the persistence of steppe communities in the inner
405 continental areas of Iberia may be associated with a reduced effective humidity, keeping
406 moisture levels below the tolerance threshold for tree growth (Tzedakis, 2007). Further
407 evidence comes from North-African palaeoenvironmental studies (Lamb et al., 1989),
408 where a strengthened monsoonal circulation has been considered as the main triggering
409 factor promoting the persistence of a regional high pressure circulation mode (Cheddadi
410 et al., 1998). In this mode, atmospheric stability and high summer temperatures may
411 have led to higher evaporation rates and a consequent reduction of water tables in many
412 continental Mediterranean areas. This mechanism may explain the prevalence of
413 reduced water levels in Iberian lakes during the early Holocene, i.e., in Lake Estanya
414 (ca. 11600-9400 cal yr BP) (Figure 8), (Morellón et al., 2009; Vegas-Vilarrúbia et al.,
415 2013). In continental Iberian sites like Salines (Roca and Julià, 1997) or Laguna de
416 Medina (Reed et al., 2001), in south-eastern Spain (Figure 1), recurrent water level
417 oscillations are revealed suggesting alternating permanent and ephemeral lake
418 environments. In Villarquemado the reduction in Pteridophytes and aquatic plants
419 (Figure 5), and the sharp decrease in siliciclastic elements (Ti, Si, Fe) contemporaneous
420 to the substantial increase in freshwater gastropoda and charophyceae-rich facies,
421 suggest an oscillation towards a shallower, carbonate-rich wetland, around 11240 cal yr
422 BP (Figure 4 and 8). The increase in Mn with respect to the LGIT values also supports

423 the existence of shallow environments where oxidation processes were more frequent.
424 The extent of the wetland was drastically reduced, as indicated by the progressive
425 decline in hygrophyte communities (Figure 6). Nevertheless, the continuous record of
426 *Tamarix*, along with the scattered presence of *Myriophyllum* and *Potamogeton*, indicate
427 the persistence of some unstable and seasonal ponds, probably in the lowest areas of the
428 basin. At the same time, the increase in Chenopodiaceae and *Artemisia* pollen may
429 reflect their local presence near the core site, in a climatic scenario with cold winter
430 temperatures hindering the development of regional meso-thermophilous vegetation
431 (Figure 6).

432 **5.1.3. Mixed oak woodland expansion during the mid Holocene (7780-5000 cal yr** 433 **BP)**

434 The mid Holocene in Villarquemado was characterized by the expansion of mesophytes
435 and Mediterranean taxa whereas *Pinus nigra/sylvestris* forests and the herbaceous
436 understory decreased (VIL-4), indicating both higher temperatures and moister
437 conditions than in the previous phase (Figure 5). Favorable conditions for forest
438 development are indicated by the dominance of *Quercus faginea* type and evergreen
439 *Quercus*, followed by the spread of broadleaved taxa, reaching their maximum values in
440 this period (Figures 5 and 8). From a regional perspective, sequences located in both
441 north (Peñalba, 1994; Sánchez Goñi and Hannon, 1999; Gil-García et al., 2002) and
442 southern slopes of the Iberian Range (Stevenson, 2000) reported similar vegetation
443 successions, where *Betula*, and to a lesser extent deciduous *Quercus*, were the most
444 widespread deciduous elements. This pattern was also found in other north-eastern
445 high-altitude localities (e.g., González-Sampériz et al. 2006; Pérez-Obiol et al. 2012;
446 Pérez-Sanz et al., 2013), reflecting an upland tree colonization associated with the
447 upward shift of the supramediterranean vegetation belt. The continuous record of *Betula*

448 pollen in Villarquemado between 10200 and 8460 cal yr BP, a taxon currently absent in
449 the area, may reflect the progressive birch colonization in the Albarracín Range as
450 highlighted by [Stevenson \(2000\)](#). *Corylus*, whose modern distribution in the Iberian
451 Peninsula is mainly related to the humid Eurosiberian region ([Blanco-Castro et al.,](#)
452 [1997](#)), was continuously recorded from ca. 9540 cal yr BP in Villarquemado, although
453 its maximum spread took place ca. 7450 cal yr BP ([Figure 5](#)), similarly to other
454 continental Iberian locations (e.g., Siles, [Carrión, 2002](#) ca. 7270 cal yr BP; Ojos del
455 Tremedal, [Stevenson, 2000](#) ca. 7500 cal yr BP).

456 The Villarquemado paleolake lowlands were most likely characterized by open
457 evergreen oak formations accompanied by scattered juniper communities in dry slopes,
458 with monospecific *Pinus pinaster* stands in redstones and an ericaceous understory
459 ([Figure 5](#)). Maximum frequencies of riparian taxa (*Alnus*, *Salix*, *Ulmus*, *Fraxinus*, *Tilia*)
460 reflect increased fluvial activity.

461 Significant *Artemisia* proportions, reaching ca. 20% despite the moister conditions,
462 could be associated with the particular geomorphological features of the basin, mainly
463 characterized by a massive spread of alluvial fans ([Figure 2A](#)), where an unstable
464 substrate might be colonized by *Artemisia* as this taxon does nowadays ([Figure 2D](#)).

465 Beyond local peculiarities, the present study matches the general hydrological model
466 established for Mediterranean Iberia, suggesting the highest lake levels occurred in the
467 8000-5500 cal yr BP period ([Carrión, 2002](#); [Morellón et al., 2009](#); [García-Alix et al.,](#)
468 [2012](#)) ([Figure 8](#)). Although a carbonate-producing wetland-shallow lake was established
469 in Villarquemado through most of the Holocene sequence, dark, organic-rich silt facies
470 with slight increases in Ti and Si occurred during the mid Holocene. Sedimentological
471 and geochemical proxies underline increased water availability during this time ([Figure](#)
472 [4](#)). Furthermore, regional-scale evidence for this wet-phase comes from tufa deposits

473 development at the Mijares River Canyon between 10000 and 5000 yr BP (Peña et al.,
474 2000), from the Guadalaviar River Basin at 7300-6800 yr BP (Sancho et al., 1997) and
475 from the headwaters of Las Parras River since 10100 cal yr BP (Rico et al., 2013)
476 (Figure 1). The increase in temperature and moisture availability recorded during this
477 period (7780-5000 cal yr BP) may be related to increased prevalence of westerlies in the
478 continental areas of the Iberian Peninsula (Benito et al., 2003), probably linked to a
479 weaker influence of the Hadley circulation system in the western Mediterranean Basin
480 (Tzedakis, 2007; Vanni ere et al., 2011).

481 A secondary change in the forest composition was observed at ca. 6800-5800 cal yr BP,
482 (VIL-4) (Figure 5). Although competition between *Quercus faginea* and evergreen
483 *Quercus* cannot be ruled out as a factor for vegetation change, the general decline of
484 mesophytes and the following increase in evergreen elements (evergreen *Quercus*, *Olea*,
485 Ericaceae) as well as the significant presence of *Pinus*, suggest a reduction of summer
486 precipitation and/or an increase of temperatures. In fact, estimates of $\delta^{13}\text{C}$ in mid
487 Holocene archaeobotanical remains located in the nearby Valencia Region confirm a
488 progressive reduction in July precipitation between 6000 and 5000 yr BP (Aguilera et
489 al., 2012). On the other hand, the reduced seasonal thermal contrast of the mid Holocene
490 caused warmer winters and milder summers, and consequently an increase in mean
491 annual temperatures allowing the spread of more thermophilous, frost-sensitive
492 elements (e.g., *Olea*, *Pistacia*, *Thymelaea*) (Figures 5 and 7) even in the inner areas of
493 the Iberian Peninsula (Badal et al., 1994; Carri on et al., 2010).

494 Regionally, the same vegetation shift from deciduous to evergreen vegetation
495 formations is reported from different continental sequences (Figure 7). At Siles, the
496 maximum expansion of the Mediterranean forest-scrub was recorded at ca. 5900 cal yr
497 BP (Carri on, 2002). At Navarr es, the colonization of sclerophyllous *Quercus* in

498 pinewoods took place around 6000 cal yr BP, possibly triggered by human-induced fires
499 under dry climate conditions (Carrión and van Geel, 1999). At Villaverde, the main
500 change towards a dominance of evergreen *Quercus* is recorded ca. 5300 cal yr BP,
501 several centuries later than other discussed records (Carrión et al., 2001) (Figure 7).
502 Anthracological data published by Allué et al., (2009) from Cova de la Guineu confirm
503 this regional-scale pattern, reporting a change from humid to sub-humid Mediterranean
504 climate, suggested by increasing abundance of evergreen *Quercus*, *Erica* and
505 *Rhamnus/Phillyrea* in the charcoal record. Although a steady increase in summer dry
506 conditions is recorded, the relatively high amount of deciduous elements especially
507 between 5800 and 5000 cal yr BP, suggests a favourable mean annual precipitation,
508 although with a more pronounced seasonality.

509 Sedimentological indicators reflect a slight decrease in lake levels with a dominance of
510 more ephemeral depositional environment that persisted through the remaining UNIT-2.

511 The change from carbonate-lake environment (SUB-2B) into shallower carbonate
512 wetland (SUB-2A) is also shown by the inverse relationship between siliciclastic
513 elements and Ca (Figure 4). This pattern towards drier conditions in continental Iberia
514 (Carrión et al., 2010a) and elsewhere in the Mediterranean Basin (Jalut et al., 2009),
515 likely represents the hydrological and vegetational response to the end of the orbitally-
516 driven African Humid Period (deMenocal et al., 2000).

517 **5.1.4. Increase in the aridity trend from the mid to late Holocene (5000-2530 cal yr** 518 **BP)**

519 Between 5000 and 2530 cal yr BP a mixed evergreen *Quercus-Pinus* forest developed
520 while *Corylus* and other mesic trees (e.g., *Fraxinus*, *Salix*, *Ulmus*), which were probably
521 confined in riverbanks and humid gorges, reduced significantly (VIL-3) (Figure 5).

522 More contrasted continental and drier climate conditions could have favoured the

523 expansion of a *Pinus*-dominated landscape at the expense of mesophytes (Carrión et al.,
524 2010a, and references therein) (Figure 5). Palynological data from areas within the
525 thermo- and mesomediterranean areas reported woodland cover reductions after ca.
526 5200 cal yr BP (Jalut et al., 2000; Pantaleón-Cano et al., 2003; Carrión, 2002; Carrión et
527 al., 2001, 2004; Fletcher et al., 2007) (Figure 8). During this period, an increase in fire
528 activity, probably enhanced by arid climate conditions, may have played a crucial role
529 in favoring the spread of sclerophyte and fire-prone communities (Carrión and van
530 Geel, 1999; Carrión et al., 2003; Gil-Romera et al., 2010a), even at high elevations
531 (Carrión et al., 2007; Anderson et al., 2011; Jiménez-Moreno and Anderson, 2012;
532 Jiménez-Moreno et al., 2013). In addition, marked changes in several lake sequences
533 took place approximately at 5100 cal yr BP. (Carrión et al., 2003; Anderson et al., 2011;
534 García-Alix et al., 2012) (Figure 8). In Villarquemado, deposition in ephemeral lake
535 conditions continued without major changes in the geochemical signature (SUB 2-A),
536 except for a significant increase in Mn that might reflect higher occurrence of oxidation
537 processes in a shallow environment (Figure 4).

538 Other pollen-independent studies reach similar conclusions: at Laguna de Medina, Reed
539 et al. (2001) suggest a clear decrease in lake levels after 5530 cal yr BP, while at Siles
540 phases of dramatic lake dessication around 5200 and 4100 cal yr BP are identified
541 (Carrión, 2002) (Figure 8). An arid interval was recorded in Lake Estanya between
542 4800-4000 cal yr BP (Morellón et al., 2009), while the sequences at Lake Zoñar
543 (Martín-Puertas et al., 2008) and Laguna de la Mula sequences (Jiménez-Moreno et al.,
544 2013) start with low lake levels at ca. 4000 cal yr BP (Figure 8). Further evidence
545 towards dry environments in continental areas of Iberia are confirmed by enhanced
546 erosive phases in the Trabaque Canyon tufa deposits (Domínguez-Villar et al., 2012),
547 and by the reduced water availability along with the consequent decline in the tufa

548 deposition in the Añavieja River system (Luzón et al., 2011). At a broader scale, the
549 spread of aridity in the southern Peninsula has been correlated with millennial and
550 submillennial-scale arid intervals in North Africa as recorded in Tigalmamine Lake
551 between 5010-4860 cal yr BP (Lamb and van der Kaars, 1995), Lake Sidi Ali at 6000-
552 5000 cal yr BP (Lamb et al., 1999) and Dar Fatma (Ben Tiba and Reille, 1982). Single
553 grains of *Cedrus* recorded in Villarquemado at the 5160-4240 cal yr BP interval suggest
554 an enhanced influence of air masses reaching northern Mediterranean areas from North
555 Africa (Magri and Parra, 2002; Di Rita and Magri, 2009).

556 **5.1.5. Clearance of pine woodlands during Iberian-Roman times (2530-1940 cal yr**
557 **BP)**

558 The continuous *Pinus* frequencies (both *Pinus sylvestris/nigra* and *Pinus*
559 *pinaster/halepensis* types) recorded in Villarquemado during the Lateglacial and the
560 Holocene until 1950 cal yr BP (Figure 5) confirm the native character of pinewoods in
561 the inner continental areas of Iberia, as shown by numerous studies (Franco-Múgica et
562 al., 2001, 2005; Carrión et al., 2004; Figueiral and Carcaillet, 2005; Rubiales et al.,
563 2009, 2011; López-Sáez et al., 2010; García-Antón et al., 2011; Morales-Molino et al.,
564 2012). *Pinus pinaster/halepensis* type is recorded throughout the record without major
565 changes, probably reflecting a long-term persistence of Mediterranean pinewoods in
566 sandy substrates of the southern Iberian Range, a region already defined by Carrión et
567 al., (2000) and recently confirmed by chloroplast microsatellite markers (Gómez et al.,
568 2005; Bucci et al., 2007), as an important source area for cluster pine during pre- and
569 postglacial times.

570 Despite the persistence of *Pinus* in our sequence, an abrupt pinewood decrease occurred
571 about ca. 2530-1940 cal yr BP, suggesting an anthropogenic disturbance (Figure 5).
572 Archaeological data and historical sources reveal that both the Celtiberian (Lorrio and

573 Ruiz-Zapatero, 2005) and Roman civilizations (Vicente-Redón, 2002) were present
574 locally, significantly altering the environment by grazing practices and building
575 structures for water management and river regulation (Rubio, 2004; Arenillas, 2007). In
576 fact, during Roman times, the Albarracín-Cella aqueduct was constructed, a magnificent
577 25 km long hydraulic infrastructure built to transfer water from the Guadalaviar River to
578 the Cella village (Almagro Gorbea, 2002) (Figure 1). Although some authors consider
579 that the aqueduct was designed by Muslim engineers (Sebastián López, 1989), the
580 discovery of high density of *terra sigillata hispanica* pottery fragments, indicates that at
581 least some parts of the infrastructure were completed before I-II A.D and therefore
582 Roman culture was present (Almagro Gorbea, 2002; Rubio, 2004). Calibrated
583 radiocarbon dates in this part of the Villarquemado sequence confirm that a major
584 change in the forest composition occurred during the Iberian-Roman Period (Figure 5).
585 Pollen evidences that the deforestation was particularly intense in the pine forest, in
586 contrast to the oak woodland (both *Quercus faginea* type and evergreen *Quercus*) that
587 surprisingly reached the highest values of the whole sequence (Figure 5). Although,
588 chronologically well-constrained, multiproxy studies have recognized the existence of a
589 moister phase between 2600 and 1600 cal yr BP, named as the Iberian-Roman Humid
590 Period (Gil-García et al., 2007; Martín-Puertas et al., 2009; Jiménez-Moreno et al.,
591 2013), the abrupt change recorded in the *Pinus* values in just 3 cm (<130 years) is
592 unlikely to be explained by climate change only. Problems linked to taphonomical
593 processes might not be relevant since the same trend is repeated in different cores from
594 Villarquemado paleolake (Figure 3A).
595 Deforestation has often been related to the intensification of agro-pastoral activities
596 (Carrion et al., 2007; López-Merino et al., 2010; Pèlachs et al., 2009a; Bal et al., 2011),
597 or mineral extraction and metallurgy (Pèlachs et al., 2009b). However, in the

598 Villarquemado sequence no agricultural intensification has been recorded during this
599 period (Figures 5 and 6) since only isolated presence of *Cerealia* type is recorded,
600 without any noticeable proportions of ruderals (e.g., *Plantago*, *Rumex*, Polygonaceae) or
601 cultivated trees (e.g., *Olea*, *Castanea*, *Juglans* and *Vitis*).

602 In addition, a preference of conifers for construction purposes compared to *Quercus* and
603 other mesophyte species has been postulated in many ethnobotanical studies (Rubiales
604 et al., 2011; Ntinou et al., 2012). *Pinus nigra* and *Pinus sylvestris* are more suitable for
605 construction as they produce straighter trunks in comparison with *Quercus ilex* which is
606 more suitable for fuelwood (Rubiales et al., 2011). Therefore, we propose that the
607 pinewood clearance recorded in Villarquemado was to obtain building material to
608 construct the Albarracín-Cella aqueduct, following the Roman economic and social
609 expansion in the area.

610 At a European scale, the climate during the Roman period (2600-1600 cal yr BP) was
611 characterized by increased humidity (van Geel et al., 1996), affecting particularly the
612 southern latitudes (Zanchetta et al., 2007). Pollen-based studies across the Iberian
613 Peninsula, especially in those regions where the human impact was substantially
614 negligible, revealed noticeable changes in the vegetation composition, with the spread
615 of deciduous elements, as recorded in Basa de la Mora (Pérez-Sanz et al., 2013), in
616 Estany de Burg (Bal et al., 2011) and Laguna de la Mula (Jiménez-Moreno et al., 2013)
617 among others. High lake productivity and the maximum diversity of the aquatic pollen
618 characterizes the Tablas de Daimiel sequence during this period (Gil-García et al., 2007)
619 coeval to the deposition of varves related to higher lake levels in Zoñar Lake (Martín-
620 Puertas et al., 2009). Although the possible forcings and the detailed chronological
621 delimitation of the mentioned period remain still unclear, the atmospheric circulation
622 pattern has been presumably related to a persistent negative NAO mode, with North

623 Atlantic origin storm tracks affecting with particular intensity south-western
624 Mediterranean areas (Martín-Puertas et al., 2012).

625 Deposition in Lake Villarquemado during the late Holocene is characterized by the co-
626 existence of carbonate wetland environments with peatbog areas. Sedimentological
627 proxies reveal a sharp change from a carbonate wetland (SUB-2A) to a peat (UNIT-1) at
628 ca. 1940 cal yr BP (Figure 4) in core VIL05-1B. However, it does not appear clearly in
629 VIL05-1A (Figure 3A), underlying the depositional spatial variability in a shallow
630 lacustrine system such as the Villarquemado paleolake.

631 ***5.1.6. Increased landscape management during the last 1500 years (1940-470 cal yr*** 632 ***BP)***

633 The time period between 1940-470 cal yr BP was characterized by the increase in
634 anthropogenic pressure shaping the current patched landscape in the Jiloca Basin.
635 Pinewoods partially recovered at high altitudes, while in the lowlands, covered by
636 evergreen and deciduous oak communities, pine reduced noticeably (VIL-1) (Figure 5).
637 Slash and burn practices were probably frequent (Figure 6) and during this period
638 livestock became an important economic activity in the area, evidenced by an
639 exponential increase in coprophilous fungi of Sordariales-group. Also, nitrophilous
640 elements like Compositae, Chenopodiaceae, *Rumex* or Apiaceae increased substantially,
641 reflecting a major change towards an open and degraded environment. Similarly,
642 *Glomus* chlamydo spores increased (Figure 6) suggesting enhanced soil erosion due to
643 grazing practices.

644 The relatively poor pollen resolution for this period together with the lack of detailed
645 geochemical analyses from the core VIL-05-1A do not allow a detailed definition of
646 climate evolution from our proxies, although it is well-known that the last two millennia
647 in the Iberian Peninsula were characterized by a marked climate variability with the

648 alternation of warm/dry and cool/moist periods (Morellón et al., 2012; Moreno et al.,
649 2012b). In general terms, deforestation ceased and pines spread in the highlands after
650 the decline of the Roman Empire (Figure 5), possibly in a drier climate context.
651 Similarly, in the nearby Albarracín Range, pinewood colonized the previous deciduous
652 woodland at 1840 cal yr BP and remained dominant until ca. 440 cal yr BP (Stevenson,
653 2000). Nevertheless, water levels seem to have remained low in the Villarquemado
654 paleolake with a patchy distribution of shallow carbonate lakes and wetlands since, no
655 major evidence of recovery is inferred from the sedimentological sequence (Figure 4) or
656 from the expansion of hygro- and hydrophyte communities (Figure 6).
657 In the 18th century, Villarquemado paleolake was artificially desiccated in order to
658 achieve new land for cultivation and/or to reduce malarial-ridden swampy areas (Rubio,
659 2004). This transition has been dated in the sedimentary sequence of Villarquemado
660 paleolake at 430 ± 30 (470 cal yr BP) radiocarbon data.

661 **5.2. Vegetation resilience to abrupt climate changes**

662 It is now well-established that the Lateglacial and Holocene periods have been
663 characterized by sharp climate changes occurring at millennial-scale (Bond et al., 1997).
664 Pollen data from central Europe have revealed an immediate response of terrestrial
665 ecosystems showing a widespread decline of drought-sensitive species such *Corylus*
666 that retreated in response to increased cool, dry and windy conditions (Tinner and
667 Lotter, 2001; Kofler et al., 2005). Similarly, the sensitivity of the Iberian vegetation to
668 global-scale climate changes has been widely reported, although it was mainly found in
669 Atlantic-influenced sequences where the vegetation succession was characterized by a
670 broadleaved vegetation expansion at the Holocene onset, shaped by short-lived peaks of
671 xerophytes, and by the progressive increase in drought tolerant taxa in response to more-
672 seasonal conditions from the mid-Holocene onwards (Carrión et al., 2010a and

673 references therein). Examples of this vegetation succession have been well-defined in
674 the Pyrenees by records such as El Portalet (González-Sampériz et al., 2006),
675 Tramacastilla (Montserrat-Martí, 1992) or by the recently published Basa de La Mora
676 (Pérez-Sánchez et al., 2013), recording marked climate shifts towards arid conditions at ca.
677 9300 and 8300 cal yr BP. Similarly, pollen data obtained from sequences located in the
678 Cantabrian Mountains (Moreno et al., 2011), in north-western Iberia (Muñoz-Sobrino et
679 al., 2005; López-Merino et al., 2012) or from coastal areas of Portugal (Fletcher et al.,
680 2007) have reported a similar vegetation succession characterized by forest opening and
681 coeval increase in steppe elements.

682 In contrast, based on a palynological approach, continental areas of the Iberian
683 Peninsula do not clearly reflect these centennial-scale climate events, even when the
684 chronological models are well-established, without apparent hiatuses and abrupt
685 changes in the sedimentation rates (e.g. Carrión and van Geel, 1999; Sánchez Goñi and
686 Hannon, 1999; Stevenson, 2000; Carrión, 2002; Carrión et al., 2007; García-Antón et
687 al., 2011) while resolution in most these cases is high enough to detect those oscillations
688 (e.g. Sánchez Goñi and Hannon, 1999; Franco-Múgica et al., 2001; Carrión, 2002;
689 Carrión et al., 2007). In Villarquemado paleolake, the depth-age model reflects a lineal,
690 continuous and relatively high sediment accumulation rate for the Lateglacial (0.030 cm
691 yr⁻¹), decreasing slightly to 0.049 cm yr⁻¹ during the early Holocene (Figure 3B).
692 Global-scale abrupt climate reversals such as the Preboreal Oscillation (Fisher et al.,
693 2002), the 8200 cal yr BP event (Alley et al., 2003), and the 4200 cal yr BP aridity crisis
694 (Cullen et al., 2000) have been chronologically well-constrained by means of
695 radiocarbon dates reporting results centered at 9820±50 (11250 cal yr BP), 7460±50
696 (8280 cal yr BP) and 3750±40 (4110 cal yr BP) respectively (Table 1). Nevertheless, no
697 major changes in the pollen sequence have been observed compared to the previous

698 trend (Figure 8). In addition, pollen analysis performed for comparison in Core VIL-05-
699 1A (not shown in this work) around the radiocarbon date 7460 ± 40 (8275 cal yr BP)
700 (Table 1) show a vegetation landscape similar to VIL-05-1B sequence, without a clear
701 evidence of forest opening around 8200 cal yr BP.

702 Considering that peculiarities related to depth-age model or sampling resolution are not
703 the main factors explaining the lack of vegetation response to abrupt events in the
704 Villarquemado paleolake, the stable character of the continental forest communities
705 could be partially explained by its optimal ecological niche, including the lack of
706 successional competitors during harsh climatic periods. Modern ecophysiological
707 studies have demonstrated that conifers are better adapted to water-stress induced by
708 drought in comparison to broadleaved trees (Lloret et al., 2007). Then, the ecosystem's
709 inertia would also play a role on buffering climate perturbations. This persistence is
710 supported by the complex interactions of the postglacial pinewoods with the newly
711 established junipers and oak forests during the recorded period. These interactions are
712 usually difficult to establish but once they are created, they hamper perturbations in
713 well-developed and mature communities (Gil-Romera et al., 2009, 2010b; Carrión et al,
714 2010b). Moreover, since aridity is an intrinsic driver of the Villarquemado landscape
715 without any clear marker of regional forest contractions during the Lateglacial and early
716 Holocene, short-lived arid spells in a drought-tolerant environment are likely to be
717 substantially negligible. This model may be extrapolated to many Iberian records that
718 see similar signals of vegetation inertia (e.g., Carrión and van Geel, 1999; Sánchez Goñi
719 and Hannon, 1999; Stevenson, 2000; Franco-Mugica et al., 2001, 2005; Carrión, 2002;
720 García-Antón et al., 2011). Instead, in Atlantic-influenced sequences the well-
721 established deciduous vegetation seems more vulnerable to arid events as the forest
722 responds showing a sharp opening or treeline experiences major shifts at high altitudes

723 that result easier to detect than in continental sequences (e.g., [Muñoz-Sobrino et al.,](#)
724 [2005;](#) [González-Sampériz et al., 2006;](#) [Moreno et al., 2011;](#) [López-Merino et al., 2012;](#)
725 [Pérez-Sáenz et al., 2013](#)). In many cases, these abrupt forest depletions are evidenced by
726 increased *Pinus* pollen frequencies indicating its xeric behaviour (e.g., [González-](#)
727 [Sampériz et al., 2006;](#) [Pérez-Sáenz et al., 2013](#)).

728 **6.- Conclusions**

729 High-resolution multiproxy analyses of the Villarquemado paleolake allow the
730 reconstruction of both meso- and supramediterranean vegetation dynamics, climate and
731 hydrological changes in the southeastern Iberian Range during the last ca. 13500 cal yr
732 BP. Most of the studied period has been characterized by a marked resilience of
733 terrestrial vegetation and gradual responses to millennial-scale climate fluctuations. The
734 main vegetation and hydrological responses to global climate variability have been
735 identified using palynological, sedimentological and geochemical indicators, enabling
736 correlations with other continental Iberian paleoenvironmental sequences. In general
737 terms, six phases occurred between ca. 13500 and 450 cal yr BP as follows:

- 738 | 1) Regional cool conditions are inferred for the LGIT (13540-11270 cal yr BP) with
739 | conifers and steppe elements as main landscape elements. In addition, the well-
740 | developed hygro-hydrophyte pollen assemblages and the sedimentary facies
741 | associations reveal high water levels, probably as a consequence of reduced
742 | evapotranspiration rates and/or higher intensity of precipitation events.
- 743 | 2) Prevalence of dry conditions in response to increased seasonality is the main feature
744 | for the early Holocene (11270-7780 cal yr BP), when conifer forests and
745 | xerophytes spread regionally. Hydrologically, this phase corresponds with an
746 | abrupt change towards a shallow carbonate-wetland with both littoral and aquatic
747 | communities experiencing a marked decrease.

- 748 3) Moister conditions characterize the beginning of the mid Holocene (7780-5000 cal
749 yr BP) in coherence with the regional pattern, showing the expansion of meso-
750 thermophilous taxa with both *Quercus faginea* and evergreen *Quercus* as main
751 woodland components. Local hydrological conditions suggest increased water
752 availability in a carbonate-wetland system.
- 753 4) The progressive increase in arid conditions during the late Holocene (5000-2530 cal
754 yr BP) enabled the expansion of a mixed *Pinus*-evergreen *Quercus* forest. The
755 carbonate-lake environment persisted during this period.
- 756 5) During Ibero-Roman times, pinewood forest clearance (2530-1940 cal yr BP)
757 represents the most important deforestation phase as a consequence of
758 anthropogenic disturbance. Carbonate shallow lakes and wetlands dominated
759 during this period and peat formation could have been favored during some
760 intervals.
- 761 6) Between 1940 and 470 cal yr BP increased landscape management associated to
762 grazing pressure shaped a patchy forest landscape without clear evidence of
763 agricultural intensification.
- 764
- 765

766 **Acknowledgments**

767 The funding for the present study derives from DINAMO (CGL-BOS 2009-07992),
768 DINAMO2 (CGL-BOS 2012-33063), IBERIAN PALEOFLORA (CGL-BOS 2012-
769 31717) and GRACCIE-CONSOLIDER (CSD2007-00067) projects, provided by the
770 Spanish Inter-Ministry Commission of Science and Technology (CICYT). Josu
771 Aranbarri acknowledges the predoctoral funding provided by the Basque Country
772 Government (ref: FI-2010-5). Ana Moreno, Graciela Gil-Romera and Mario Morellón
773 hold post-doctoral contracts funded by “Ramon y Cajal (ref: RYC-2008-02431)”, “Juan
774 de la Cierva (ref: JCI2009-04345)” and “JAE DOC CSIC (ref: JAEDOC-2011-026)”
775 programmes, respectively. Eduardo García-Prieto is supported by a predoctoral FPI grant
776 (BES-2010-038593). We are very grateful to Aida Adsuar, Beatriz Bueno and Raquel
777 López-Cantero for their assistance in core sampling and laboratory procedures. Josu
778 Aranbarri thanks colleagues from the Dipartimento di Biologia Ambientale, especially
779 Alessandra Celant, for continuous encouragement. We would also like to thank Thomas
780 M. Cronin, Anthony C. Stevenson and an anonymous reviewer for their valuable
781 suggestions.

782

783

784

785

786

787

788

789

790

791 **References**

- 792 Aguilera, M., Ferrio, J.P., Pérez, G., Araus, J.L., Voltas, J., 2012. Holocene changes in
793 precipitation seasonality in the western Mediterranean Basin: a multi-species approach
794 using $\delta^{13}\text{C}$ of archaeobotanical remains. *Journal of Quaternary Science* 27, 192-202.
795
- 796 Ali, A.A., Carcaillet, C., Guendon, J.-L., Quinif, Y., Roiron, P., Terral, J.-F., 2003. The
797 Early Holocene treeline in the southern French Alps: new evidence from travertine
798 formations. *Global Ecology and Biogeography* 12, 411-419.
799
- 800 Alley, R.B., Mayewski, P.A., Sowers, T., Stuiver, M., Taylor, K.C., Clark, P.U., 1997.
801 Holocene climatic instability: A prominent, widespread event 8200 yr ago. *Geology* 25,
802 483-486.
803
- 804 Alley, R.B., Marotzke, J., Nordhaus, W.D., Overpeck, J.T., Peteet, D.M., Pielke, R.A.,
805 Pierrehumbert, R.T., Rhines, P.B., Stocker, T.F., Talley, L.D., Wallace, J.M., 2003.
806 Abrupt Climate Change. *Science* 299, 2005-2010.
807
- 808 Allué, E., Vernet, J.-L., Cebrià, A., 2009. Holocene vegetational landscapes of NE
809 Iberia: charcoal analysis from Cova de la Guineu, Barcelona, Spain. *The Holocene* 19,
810 765-773.
811
- 812 Almagro Gorbea, A., 2002. Acueducto de Albarracín a Cella (Teruel). *Ingeniería*
813 *romana en España*. Madrid, 213-237.
814
- 815 Anderson, R.S., Jiménez-Moreno, G., Carrión, J.S., Pérez-Martínez, C., 2011.
816 Postglacial history of alpine vegetation, fire, and climate from Laguna de Río Seco,
817 Sierra Nevada, southern Spain. *Quaternary Science Reviews* 30, 1615-1629.
818
- 819 Arenillas, M., 2007. A Brief History of Water Projects in Aragon. *International Journal*
820 *of Water Resources Development* 23, 189-204.
821
- 822 Aura, J.E., Jordá, J.F., Montes, L., Utrilla, P., 2011. Human responses to Younger Dryas
823 in the Ebro valley and Mediterranean watershed (Eastern Spain). *Quaternary*
824 *International* 242, 348-359.
825
- 826 Badal, E., Bernabeu, J., Vernet, J.L., 1994. Vegetation changes and human action from
827 the Neolithic to the Bronze Age (7000–4000 B.P.) in Alicante, Spain, based on charcoal
828 analysis. *Vegetation History and Archaeobotany* 3, 155-166.
829
- 830 Bal, M.-C., Pèlachs, A., Pérez-Obiol, R., Julià, R., Cunill, R., 2011. Fire history and
831 human activities during the last 3300 cal yr BP in Spain's Central Pyrenees: The case of
832 the Estany de Burg. *Palaeogeography, Palaeoclimatology, Palaeoecology* 300, 179-190.
833
- 834 Barreiro-Lostres, F., Moreno, A., Giralt, S., Valero-Garcés, B.L., 2013. Evolución
835 sedimentaria del lago kárstico de La Parra (Cuenca) durante los últimos 1600 años:
836 paleohidrología, clima e impacto humano. *Cuadernos de Investigación Geográfica* 39,
837 179-193.
838

839 Benito, G., Sopena, A., Sánchez-Moya, Y., Machado, M.J., Pérez-González, A., 2003.
840 Palaeoflood record of the Tagus River (Central Spain) during the Late Pleistocene and
841 Holocene. *Quaternary Science Reviews* 22, 1737-1756.
842
843 Bennett, K., 2009. Documentation for Psimpoll 4.27 and Pscomb 1.03: C Programs for
844 Plotting Pollen Diagrams and Analysing Pollen Data, Queen's University of Belfast,
845 Department of Archaeology and Palaeoecology.
846
847 Ben Tiba, B., Reille, M., 1982. Recherches pollen-analytiques dans les montagnes de
848 Kroumirie (Tunisie septentrionale): premiers résultats. *Ecologia Mediterranea* 8, 75-86.
849
850 Björck, S., Rundgren, M., Ingólfsson, Ó., Funder, S., 1997. The Preboreal oscillation
851 around the Nordic Seas: terrestrial and lacustrine responses. *Journal of Quaternary*
852 *Science* 12, 455-465.
853
854 Blaauw, M., 2010. Methods and code for "classical" age-modelling of radiocarbon
855 sequences. *Quaternary Geochronology* 5, 512-518.
856
857 Blanco-Castro, E., Casado, M., Costa, M., Escribano, R., García-Antón, M., Génova,
858 M., Gómez, A., Moreno, J., Morla, C., Regato, P., Sainz Ollero, H., 1997. Los bosques
859 ibéricos. Una interpretación geobotánica. Barcelona, Planeta 572.
860
861 Bond, G., Showers, W., Cheseby, M., Lotti, R., Almasi, P., deMenocal, P., Priore, P.,
862 Cullen, H., Hajdas, I., Bonani, G., 1997. A Pervasive Millennial-Scale Cycle in North
863 Atlantic Holocene and Glacial Climates. *Science* 278, 1257-1266.
864
865 Bucci, G., González-Martínez, S.C., Le Provost, G., Plomion, C., Ribeiro, M.M.,
866 Sebastiani, F., Alía, R., Vendramin, G.G., 2007. Range-wide phylogeography and gene
867 zones in *Pinus pinaster* Ait. revealed by chloroplast microsatellite markers. *Molecular*
868 *Ecology* 16, 2137-2153.
869
870 Cacho, I., Grimalt, J.O., Canals, M., Sbaiffi, L., Shackleton, N.J., Schönfeld, J., Zahn,
871 R., 2001. Variability of the western Mediterranean Sea surface temperature during the
872 last 25,000 years and its connection with the Northern Hemisphere climatic changes.
873 *Paleoceanography* 16, 40-52.
874
875 Carrión, J.S., 2002. Patterns and processes of Late Quaternary environmental change in
876 a montane region of southwestern Europe. *Quaternary Science Reviews* 21, 2047-2066.
877
878 Carrión, J.S., van Geel, B., 1999. Fine-resolution Upper Weichselian and Holocene
879 palynological record from Navarrés (Valencia, Spain) and a discussion about factors of
880 Mediterranean forest succession. *Review of Palaeobotany and Palynology* 106, 209-
881 236.
882
883 Carrión, J.S., Navarro, C., Navarro, J., Munuera, M., 2000. The distribution of cluster
884 pine (*Pinus pinaster*) in Spain as derived from palaeoecological data: relationships with
885 phytosociological classification. *The Holocene* 10, 243-252.
886

887 Carrión, J.S., Andrade, A., Bennett, K.D., Navarro, C., Munuera, M., 2001. Crossing
888 forest thresholds: inertia and collapse in a Holocene sequence from south-central Spain.
889 The Holocene 11, 635-653.
890

891 Carrión, J.S., Sánchez-Gómez, P., Mota, J.F., Yll, R., Chaín, C., 2003. Holocene
892 vegetation dynamics, fire and grazing in the Sierra de Gádor, southern Spain. The
893 Holocene 13, 839-849.
894

895 Carrión, J.S., Yll, E.I., Willis, K.J., Sánchez, P., 2004. Holocene forest history of the
896 eastern plateaux in the Segura Mountains (Murcia, southeastern Spain). Review of
897 Palaeobotany and Palynology 132, 219-236.
898

899 Carrión, J.S., Fuentes, N., González-Sampériz, P., Sánchez Quirante, L., Finlayson,
900 J.C., Fernández, S., Andrade, A., 2007. Holocene environmental change in a montane
901 region of southern Europe with a long history of human settlement. Quaternary Science
902 Reviews 26, 1455-1475.
903

904 Carrión, J.S., Fernández, S., González-Sampériz, P., Gil-Romera, G., Badal, E.,
905 Carrión-Marco, Y., López-Merino, L., López-Sáez, J.A., Fierro, E., Burjachs, F., 2010a.
906 Expected trends and surprises in the Lateglacial and Holocene vegetation history of the
907 Iberian Peninsula and Balearic Islands. Review of Palaeobotany and Palynology 162,
908 458-475.
909

910 Carrión, J.S., Fernández, S., Jiménez-Moreno, G., Fauquette, S., Gil-Romera, G.,
911 González-Sampériz, P., Finlayson, C., 2010b. The historical origins of aridity and
912 vegetation degradation in southeastern Spain. Journal of Arid Environments 74, 731-
913 736.
914

915 Carrión, Y., Ntinou, M., Badal, E., 2010. *Olea europaea* L. in the North Mediterranean
916 Basin during the Pleniglacial and the Early-Middle Holocene. Quaternary Science
917 Reviews 29, 952-968.
918

919 Casas-Sainz, A.M., De Vicente, G., 2009. On the tectonic origin of Iberian topography.
920 Tectonophysics 474, 214-235.
921

922 Combourieu Nebout, N., Peyron, O., Dormoy, I., Desprat, S., Beaudouin, C., Kotthoff,
923 U., Marret, F., 2009. Rapid climatic variability in the west Mediterranean during the last
924 25 000 years from high resolution pollen data. Climate of the Past 5, 503-521.
925

926 Constante, A., Peña, J.L., Muñoz, A., Picazo, J., 2011. Climate and anthropogenic
927 factors affecting alluvial fan development during the late Holocene in the central Ebro
928 Valley, northeast Spain. The Holocene 21, 275-286.
929

930 Cortés-Sánchez, M., Jiménez Espejo, F.J., Simón Vallejo, M.D., Gibaja Bao, J.F.,
931 Carvalho, A.F., Martínez-Ruiz, F., Gamiz, M.R., Flores, J.-A., Paytan, A., López Sáez,
932 J.A., Peña-Chocarro, L., Carrión, J.S., Morales Muñiz, A., Roselló Izquierdo, E.,
933 Riquelme Cantal, J.A., Dean, R.M., Salgueiro, E., Martínez Sánchez, R.M., De la Rubia
934 de Gracia, J.J., Lozano Francisco, M.C., Vera Peláez, J.L., Rodríguez, L.L., Bicho,
935 N.F., 2012. The Mesolithic-Neolithic transition in southern Iberia. Quaternary Research
936 77, 221-234.

937
938 Cullen, H.M., deMenocal, P.B., Hemming, S., Hemming, G., Brown, F.H., Guilderson,
939 T., Sirocko, F., 2000. Climate change and the collapse of the Akkadian empire:
940 evidence from the deep sea. *Geology* 28, 379-382.
941
942 Cheddadi, R., Lamb, H.F., Guiot, J., Van Der Kaars, S., 1998. Holocene climatic
943 change in Morocco: a quantitative reconstruction from pollen data. *Climate Dynamics*
944 14, 883-890.
945
946 Davis, B.A.S., Stevenson, A.C., 2007. The 8.2 ka event and Early–Mid Holocene
947 forests, fires and flooding in the Central Ebro Desert, NE Spain. *Quaternary Science*
948 *Reviews* 26, 1695-1712.
949
950 deMenocal, P., Ortiz, J., Guilderson, T., Adkins, J., Sarnthein, M., Baker, L.,
951 Yarusinsky, M., 2000. Abrupt onset and termination of the African Humid Period: rapid
952 climate responses to gradual insolation forcing. *Quaternary Science Reviews* 19, 347-
953 361.
954
955 Denton, G.H., Broecker, W.S., 2008. Wobbly ocean conveyor circulation during the
956 Holocene? *Quaternary Science Reviews* 27, 1939-1950.
957
958 Di Rita, F., Magri, D., 2009. Holocene drought, deforestation and evergreen vegetation
959 development in the central Mediterranean: a 5500 year record from Lago Alimini
960 Piccolo, Apulia, southeast Italy. *The Holocene* 19, 295-306.
961
962 Domínguez-Villar, D., Vázquez-Navarro, J.A., Carrasco, R.M., 2012. Mid-Holocene
963 erosive episodes in tufa deposits from Trabaque Canyon, central Spain, as a result of
964 abrupt arid climate transitions. *Geomorphology* 161-162, 15–25.
965
966 Figueiral, I., Carcaillet, C., 2005. A review of Late Pleistocene and Holocene
967 biogeography of highland Mediterranean pines (*Pinus* type *sylvestris*) in Portugal, based
968 on wood charcoal. *Quaternary Science Reviews* 24, 2466-2476.
969
970 Fisher, T.G., Smith, D.G., Andrews, J.T., 2002. Preboreal oscillation caused by a glacial
971 Lake Agassiz flood. *Quaternary Science Reviews* 21, 873-878.
972
973 Fletcher, W.J., Boski, T., Moura, D., 2007. Palynological evidence for environmental
974 and climatic change in the lower Guadiana valley, Portugal, during the last 13 000
975 years. *The Holocene* 17, 481-494.
976
977 Fletcher, W.J., Sánchez Goñi, M.F., 2008. Orbital- and sub-orbital-scale climate
978 impacts on vegetation of the western Mediterranean basin over the last 48,000 yr.
979 *Quaternary Research* 70, 451-464.
980
981 Fletcher, W.J., Sánchez Goñi, M.F., Peyron, O., Dormoy, I., 2010. Abrupt climate
982 changes of the last deglaciation detected in a western Mediterranean forest record.
983 *Climate of the Past* 6, 245-264.
984

- 985 Franco-Múgica, F., García-Antón, M., Maldonado-Ruiz, J., Morla-Juaristi, C., Sainz-
986 Ollero, H., 2001. The Holocene history of *Pinus* forests in the Spanish Northern Meseta.
987 *The Holocene* 11, 343-358.
988
- 989 Franco-Múgica, F., García-Antón, M., Maldonado-Ruiz, J., Morla-Juaristi, C., Sainz-
990 Ollero, H., 2005. Ancient pine forest on inland dunes in the Spanish northern meseta.
991 *Quaternary Research* 63, 1-14.
992
- 993 Frigola, J., Moreno, A., Cacho, I., Canals, M., Sierro, F.J., Flores, J.A., Grimalt, J.O.,
994 Hodell, D.A., Curtis, J.H., 2007. Holocene climate variability in the western
995 Mediterranean region from a deepwater sediment record. *Paleoceanography* 22.
996
- 997 García-Alix, A., Jiménez-Moreno, G., Anderson, R.S., Jiménez-Espejo, F.J., Delgado-
998 Huertas, A., 2012. Holocene environmental change in southern Spain deduced from the
999 isotopic record of a high-elevation wetland in Sierra Nevada. *Journal of Paleolimnology*
1000 48, 471-484.
1001
- 1002 García-Antón, M., Franco-Múgica, F., Morla-Juaristi, C., Maldonado-Ruiz, J., 2011.
1003 The biogeographical role of *Pinus* forest on the Northern Spanish Meseta: a new
1004 Holocene sequence. *Quaternary Science Reviews* 30, 757-768.
1005
- 1006 Gil-García, M.J., Dorado-Valiño, M., Valdeolmillos Rodríguez, A., Ruíz-Zapata, M.B.,
1007 2002. Late-glacial and Holocene palaeoclimatic record from Sierra de Cebollera
1008 (northern Iberian Range, Spain). *Quaternary International* 93-94, 13-18.
1009
- 1010 Gil-García, M.J., Ruiz-Zapata, M.B., Santisteban, J.I., Mediavilla, R., López-Pamo, E.,
1011 Dabrio, C.J., 2007. Late holocene environments in Las Tablas de Daimiel (south central
1012 Iberian peninsula, Spain). *Vegetation History and Archaeobotany* 16, 241-250.
1013
- 1014 Gil-Romera, G., Carrión, J.S., McClure, S.B., Schmich, S., Finlayson, C., 2009.
1015 Holocene vegetation dynamics in mediterranean Iberia: Historical contingency and
1016 climate-human interactions. *Journal of Anthropological Research* 65, 271-285.
1017
- 1018 Gil-Romera, G., Carrión, J.S., Pausas, J.G., Sevilla-Callejo, M., Lamb, H.F., Fernández,
1019 S., Burjachs, F., 2010a. Holocene fire activity and vegetation response in South-Eastern
1020 Iberia. *Quaternary Science Reviews* 29, 1082-1092.
1021
- 1022 Gil-Romera, G., López-Merino, L., Carrión, J.S., González-Sampériz, P., Martín-
1023 Puertas, C., López-Sáez J.A., Fernández, S., García-Antón, M., Stefanova, V., 2010b.
1024 Interpreting resilience through long-term ecology: Potential insights in western
1025 Mediterranean landscapes. *Open Ecology Journal*, 3, 43-53.
1026
- 1027 Gómez, A., Vendramin, G.G., González-Martínez, S.C., Alía, R., 2005. Genetic
1028 diversity and differentiation of two Mediterranean pines (*Pinus halepensis* Mill. and
1029 *Pinus pinaster* Ait.) along a latitudinal cline using chloroplast microsatellite markers.
1030 *Diversity and Distributions* 11, 257-263.
1031
- 1032 González-Sampériz, P., Valero-Garcés, B.L., Carrión, J.S., Peña-Monné, J.L., García-
1033 Ruiz, J.M., Martí-Bono, C., 2005. Glacial and Lateglacial vegetation in northeastern
1034 Spain: New data and a review. *Quaternary International* 140-141, 4-20.

1035
1036 González-Sampérez, P., Valero-Garcés, B.L., Moreno, A., Jalut, G., García-Ruiz, J.M.,
1037 Martí-Bono, C., Delgado-Huertas, A., Navas, A., Otto, T., Dedoubat, J.J., 2006. Climate
1038 variability in the Spanish Pyrenees during the last 30,000 yr revealed by the El Portalet
1039 sequence. *Quaternary Research* 66, 38-52.
1040
1041 González-Sampérez, P., Valero-Garcés, B.L., Moreno, A., Morellón, M., Navas, A.,
1042 Machín, J., Delgado-Huertas, A., 2008. Vegetation changes and hydrological
1043 fluctuations in the Central Ebro Basin (NE Spain) since the Late Glacial period: Saline
1044 lake records. *Palaeogeography, Palaeoclimatology, Palaeoecology* 259, 157-181.
1045
1046 González-Sampérez, P., Utrilla, P., Mazo, C., Valero-Garcés, B., Sopena, M., Morellón,
1047 M., Sebastián, M., Moreno, A., Martínez-Bea, M., 2009. Patterns of human occupation
1048 during the early Holocene in the Central Ebro Basin (NE Spain) in response to the
1049 8.2 ka climatic event. *Quaternary Research* 71, 121-132.
1050
1051 González-Sampérez, P., Leroy, S.A.G., Carrión, J.S., Fernández, S., García-Antón, M.,
1052 Gil-García, M.J., Uzquiano, P., Valero-Garcés, B., Figueiral, I., 2010. Steppes,
1053 savannahs, forests and phytodiversity reservoirs during the Pleistocene in the Iberian
1054 Peninsula. *Review of Palaeobotany and Palynology* 162, 427-457.
1055
1056 González-Sampérez, P., García-Prieto, E., Aranbarri, J., Valero-Garcés, B.L., Moreno,
1057 A., Gil-Romera, G., Sevilla-Callejo, M., Santos, L., Morellón, M., Mata, P., Andrade,
1058 A., Carrión, J.S., 2013. Reconstrucción paleoambiental del último ciclo glacial en la
1059 Iberia continental: la secuencia del Cañizar de Villarquemado (Teruel). *Cuadernos de*
1060 *Investigación Geográfica* 39, 49-76.
1061
1062 Gracia, F.J., Gutiérrez, F., Gutiérrez, M., 2003. The Jiloca karst polje-tectonic graben
1063 (Iberian Range, NE Spain). *Geomorphology* 52, 215-231.
1064
1065 Grimm, E.C., 1987. CONISS: a Fortran 77 program for stratigraphically constrained
1066 cluster analysis by the method of incremental sum of squares. *Computers &*
1067 *Geosciences* 13, 3-35.
1068
1069 Gutiérrez, F., Valero-Garcés, B., Desir, G., González-Sampérez, P., Gutiérrez, M.,
1070 Linares, R., Zarroca, M., Moreno, A., Guerrero, J., Roqué, C., Arnold, L.J., Demuro,
1071 M., 2013. Late Holocene evolution of playa lakes in the central Ebro depression based
1072 on geophysical surveys and morpho-stratigraphic analysis of lacustrine terraces.
1073 *Geomorphology* 196, 177-197.
1074
1075 Gutiérrez-Elorza, M., Gracia, F.J., 1997. Environmental interpretation and evolution of
1076 the Tertiary erosion surfaces in the Iberian Range (Spain). Geological Society, London,
1077 *Special Publications* 120, 147-158.
1078
1079 Hammer, O., Harper, D.A.T., Ryan, P.D., 2001. PAST: Paleontological Statistics
1080 Software Package for Education and Data Analysis. *Palaeontologia Electronica* 4.
1081
1082 Hoek, W.Z., Yu, Z.C., Lowe, J.J., 2008. INTegration of Ice-core, MARine, and
1083 TERrestrial records (INTIMATE): refining the record of the Last Glacial–Interglacial
1084 Transition. *Quaternary Science Reviews* 27, 1-5.

1085
1086 Jalut, G., Esteban Amat, A., Bonnet, L., Gauquelin, T., Fontugne, M., 2000. Holocene
1087 climatic changes in the Western Mediterranean, from south-east France to south-east
1088 Spain. *Palaeogeography, Palaeoclimatology, Palaeoecology* 160, 255-290.
1089
1090 Jalut, G., Dedoubat, J.J., Fontugne, M., Otto, T., 2009. Holocene circum-Mediterranean
1091 vegetation changes: Climate forcing and human impact. *Quaternary International* 200,
1092 4-18.
1093
1094 Jiménez-Moreno, G., Anderson, R.S., 2012. Holocene vegetation and climate change
1095 recorded in alpine bog sediments from the Borreguiles de la Virgen, Sierra Nevada,
1096 southern Spain. *Quaternary Research* 77, 44-53.
1097
1098 Jiménez-Moreno, G., García-Alix, A., Hernández-Corbalán, M.D., Anderson, R.S.,
1099 Delgado-Huertas, A., 2013. Vegetation, fire, climate and human disturbance history in
1100 the southwestern Mediterranean area during the late Holocene. *Quaternary Research* 79,
1101 110-122.
1102
1103 Kim, J.-H., Rimbu, N., Lorenz, S.J., Lohmann, G., Nam, S.-I., Schouten, S.,
1104 Rühlemann, C., Schneider, R.R., 2004. North Pacific and North Atlantic sea-surface
1105 temperature variability during the Holocene. *Quaternary Science Reviews* 23, 2141-
1106 2154.
1107
1108 Kofler, W., Krapf, V., Oberhuber, W., Bortenschlager, S., 2005. Vegetation responses
1109 to the 8200 cal. BP cold event and to long-term climatic changes in the Eastern Alps:
1110 possible influence of solar activity and North Atlantic freshwater pulses. *The Holocene*
1111 15, 779-788.
1112
1113 Kullman, L., 2013. Ecological tree line history and palaeoclimate - review of megafossil
1114 evidence from the Swedish Scandes. *Boreas* 42, 555-567.
1115
1116 Lamb, H.F., Eicher, U., Switsur, V.R., 1989. An 18,000-Year Record of Vegetation,
1117 Lake-Level and Climatic Change from Tigmamine, Middle Atlas, Morocco. *Journal*
1118 *of Biogeography* 16, 65-74.
1119
1120 Lamb, H.F., van der Kaars, S., 1995. Vegetational response to Holocene climatic
1121 change: pollen and palaeolimnological data from the Middle Atlas, Morocco. *The*
1122 *Holocene* 5, 400-408.
1123
1124 Lamb, H., Roberts, N., Leng, M., Barker, P., Benkaddour, A., van der Kaars, S., 1999.
1125 Lake evolution in a semi-arid montane environment: response to catchment change and
1126 hydroclimatic variation. *Journal of Paleolimnology* 21, 325-343.
1127
1128 Lloret, F., Lobo, A., Estevan, H., Maisongrande, P., Vayreda, J., Terradas, J., 2007.
1129 Woody plant richness and NDVI response to drought events in Catalanian (northeastern
1130 Spain) forests. *Ecology* 88, 2270-2279.
1131
1132 López-Blanco, C., Gaillard, M.-J., Miracle, M.R., Vicente, E., 2012. Lake-level changes
1133 and fire history at Lagunillo del Tejo (Spain) during the last millennium: Climate or
1134 human impact? *The Holocene* 22, 551-560.

1135
1136 López-Merino, L., Martínez Cortizas, A., López-Sáez, J.A., 2010. Early agriculture and
1137 palaeoenvironmental history in the North of the Iberian Peninsula: a multi-proxy
1138 analysis of the Monte Areo mire (Asturias, Spain). *Journal of Archaeological Science*
1139 *37*, 1978-1988.
1140
1141 López-Merino, L., Silva Sánchez, N., Kaal, J., López-Sáez, J.A., Martínez Cortizas, A.,
1142 2012. Post-disturbance vegetation dynamics during the Late Pleistocene and the
1143 Holocene: An example from NW Iberia. *Global and Planetary Change* *92-93*, 58-70.
1144
1145 López-Sáez, J.A., López-Merino, L., Alba-Sánchez, F., Pérez-Díaz, S., Abel-Schaad,
1146 D., Carrión, J.S., 2010. Late Holocene ecological history of *Pinus pinaster* forests in the
1147 Sierra de Gredos of central Spain. *Plant Ecology* *206*, 195-209.
1148
1149 Lorrio, A.J., Ruiz-Zapatero, G., 2005. The Celts in Iberia: an overview. *Journal of*
1150 *Interdisciplinary Celtic Studies* *6*, 1-88.
1151
1152 Lowe, J.J., Rasmussen, S.O., Björck, S., Hoek, W.Z., Steffensen, J.P., Walker, M.J.C.,
1153 Yu, Z.C., 2008. Synchronisation of palaeoenvironmental events in the North Atlantic
1154 region during the Last Termination: a revised protocol recommended by the
1155 INTIMATE group. *Quaternary Science Reviews* *27*, 6-17.
1156
1157 Luzón, A., Pérez, A., Mayayo, M.J., Soria, A.R., Sánchez Goñi, M.F., Roc, A.C., 2007.
1158 Holocene environmental changes in the Gallocanta lacustrine basin, Iberian Range, NE
1159 Spain. *The Holocene* *17*, 649-663.
1160
1161 Luzón, M.A., Pérez, A., Borrego, A.G., Mayayo, M.J., Soria, A.R., 2011. Interrelated
1162 continental sedimentary environments in the central Iberian Range (Spain): Facies
1163 characterization and main palaeoenvironmental changes during the Holocene.
1164 *Sedimentary Geology* *239*, 87-103.
1165
1166 Magri, D., Parra, I., 2002. Late Quaternary western Mediterranean pollen records and
1167 African winds. *Earth and Planetary Science Letters* *200*, 401-408.
1168
1169 Martín-Puertas, C., Valero-Garcés, B.L., Mata, M.P., González-Sampéiz, P., Bao, R.,
1170 Moreno, A., Stefanova, V., 2008. Arid and humid phases in southern Spain during the
1171 last 4000 years: the Zoñar Lake record, Córdoba. *The Holocene* *18*, 907-921.
1172
1173 Martín-Puertas, C., Valero-Garcés, B.L., Brauer, A., Mata, M.P., Delgado-Huertas, A.,
1174 Dulski, P., 2009. The Iberian–Roman Humid Period (2600–1600 cal yr BP) in the Zoñar
1175 Lake varve record (Andalucía, southern Spain). *Quaternary Research* *71*, 108-120.
1176
1177 Martín-Puertas, C., Matthes, K., Brauer, A., Muscheler, R., Hansen, F., Petrick, C.,
1178 Aldahan, A., Possnert, G., van Geel, B., 2012. Regional atmospheric circulation shifts
1179 induced by a grand solar minimum. *Nature Geoscience* *5*, 397-401.
1180
1181 Mayewski, P.A., Rohling, E.E., Curt Stager, J., Karlén, W., Maasch, K.A., David
1182 Meeker, L., Meyerson, E.A., Gasse, F., van Kreveld, S., Holmgren, K., Lee-Thorp, J.,
1183 Rosqvist, G., Rack, F., Staubwasser, M., Schneider, R.R., Steig, E.J., 2004. Holocene
1184 climate variability. *Quaternary Research* *62*, 243-255.

1185
1186 Montserrat-Martí, J., 1992. Evolución glaciario y postglaciario del clima y la vegetación en
1187 la vertiente sur del Pirineo: estudio palinológico. Monografías del Instituto Pirenaico de
1188 Ecología-CSIC, Zaragoza.
1189
1190 Moore, P., Webb, J.A., Collinson, A., 1991. Pollen Analysis, second ed. Blackwell
1191 Scientific Publications, Oxford.
1192
1193 Morales-Molino, C., Postigo-Mijarra, J.M., Morla, C., García-Antón, M., 2012. Long-
1194 term persistence of Mediterranean pine forests in the Duero Basin (central Spain) during
1195 the Holocene: The case of *Pinus pinaster* Aiton. *The Holocene* 22, 561-570.
1196
1197 Morellón, M., Valero-Garcés, B., Vegas-Vilarrúbia, T., González-Sampériz, P.,
1198 Romero, Ó., Delgado-Huertas, A., Mata, P., Moreno, A., Rico, M., Corella, J.P., 2009.
1199 Lateglacial and Holocene palaeohydrology in the western Mediterranean region: The
1200 Lake Estanya record (NE Spain). *Quaternary Science Reviews* 28, 2582-2599.
1201
1202 Morellón, M., Pérez-Sanz, A., Corella, J.P., Büntgen, U., Catalán, J., González-
1203 Sampériz, P., González-Trueba, J.J., López-Sáez, J.A., Moreno, A., Pla-Rabes, S., Saz-
1204 Sánchez, M. á., Scussolini, P., Serrano, E., Steinhilber, F., Stefanova, V., Vegas-
1205 Vilarrúbia, T., Valero-Garcés, B., 2012. A multi-proxy perspective on millennium-long
1206 climate variability in the Southern Pyrenees. *Climate of the Past* 8, 683-700.
1207
1208 Moreno, A., Valero-Garcés, B.L., González-Sampériz, P., Rico, M., 2008. Flood
1209 response to rainfall variability during the last 2000 years inferred from the Taravilla
1210 Lake record (Central Iberian Range, Spain). *Journal of Paleolimnology* 40, 943-961.
1211
1212 Moreno, A., Stoll, H., Jiménez-Sánchez, M., Cacho, I., Valero-Garcés, B., Ito, E.,
1213 Edwards, R.L., 2010. A speleothem record of glacial (25–11.6 kyr BP) rapid climatic
1214 changes from northern Iberian Peninsula. *Global and Planetary Change* 71, 218-231.
1215
1216 Moreno, A., López-Merino, L., Leira, M., Marco-Barba, J., González-Sampériz, P.,
1217 Valero-Garcés, B.L., López-Sáez, J.A., Santos, L., Mata, P., Ito, E., 2011. Revealing the
1218 last 13,500 years of environmental history from the multiproxy record of a mountain
1219 lake (Lago Enol, northern Iberian Peninsula). *Journal of Paleolimnology* 46, 327-349.
1220
1221 Moreno, A., González-Sampériz, P., Morellón, M., Valero-Garcés, B.L., Fletcher, W.J.,
1222 2012a. Northern Iberian abrupt climate change dynamics during the last glacial cycle: A
1223 view from lacustrine sediments. *Quaternary Science Reviews* 36, 139-153.
1224
1225 Moreno, A., Pérez, A., Frigola, J., Nieto-Moreno, V., Rodrigo-Gámiz, M., Martrat, B.,
1226 González-Sampériz, P., Morellón, M., Martín-Puertas, C., Corella, J.P., Belmonte, Á.,
1227 Sancho, C., Cacho, I., Herrera, G., Canals, M., Grimalt, J.O., Jiménez-Espejo, F.,
1228 Martínez-Ruiz, F., Vegas-Vilarrúbia, T., Valero-Garcés, B.L., 2012b. The Medieval
1229 Climate Anomaly in the Iberian Peninsula reconstructed from marine and lake records.
1230 *Quaternary Science Reviews* 43, 16-32.
1231
1232 Muñoz Sobrino, C., Ramil-Rego, P., Gómez-Orellana, L., Varela, R.A.D., 2005.
1233 Palynological data on major Holocene climatic events in NW Iberia. *Boreas* 34, 381-
1234 400.

1235
1236 Muñoz Sobrino, C., Heiri, O., Hazekamp, M., van der Velden, D., Kirilova, E.P.,
1237 García-Moreiras, I., Lotter, A.F., 2013. New data on the Lateglacial period of SW
1238 Europe: a high resolution multiproxy record from Laguna de la Roya (NW Iberia).
1239 Quaternary Science Reviews 80, 58-77.
1240
1241 Ntinou, M., Badal, E., Carrión, Y., Fueyo, J.L.M., Carrión, R.F., Mira, J.P., 2013. Wood
1242 use in a medieval village: the contribution of wood charcoal analysis to the history of
1243 land use during the 13th and 14th centuries a.d. at Pobla d'Ifach, Calp, Alicante, Spain.
1244 Vegetation History and Archaeobotany 22, 115-128.
1245
1246 Pantaléon-Cano, J., Yll, E.-I., Pérez-Obiol, R., Roure, J.M., 2003. Palynological
1247 evidence for vegetational history in semi-arid areas of the western Mediterranean
1248 (Almería, Spain). The Holocene 13, 109-119.
1249
1250 Pèlachs, A., Nadal, J., Soriano, J.M., Molina, D., Cunill, R., 2009a. Changes in
1251 Pyrenean woodlands as a result of the intensity of human exploitation: 2,000 years of
1252 metallurgy in Vallferrera, northeast Iberian Peninsula. Vegetation History and
1253 Archaeobotany 18, 403-416.
1254
1255 Pèlachs, A., Pérez-Obiol, R., Ninyerola, M., Nadal, J., 2009b. Landscape dynamics of
1256 *Abies* and *Fagus* in the southern Pyrenees during the last 2200 years as a result of
1257 anthropogenic impacts. Review of Palaeobotany and Palynology 156, 337-349.
1258
1259 Peña, J. L., Sancho, C., Lozano, M. V., 2000. Climatic and tectonic significance of Late
1260 Pleistocene and Holocene tufa deposits in the Mijares River canyon, eastern Iberian
1261 Range, northeast Spain. Earth Surface Processes and Landforms 25, 1403-1417.
1262
1263 Peñalba, M.C., 1994. The History of the Holocene Vegetation in Northern Spain from
1264 Pollen Analysis. Journal of Ecology 82, 815-832.
1265
1266 Pérez-Obiol, R., Julià, R., 1994. Climatic Change on the Iberian Peninsula Recorded in
1267 a 30,000-Yr Pollen Record from Lake Banyoles. Quaternary Research 41, 91-98.
1268
1269 Pérez-Obiol, R., Bal, M.-C., Pèlachs, A., Cunill, R., Soriano, J.M., 2012. Vegetation
1270 dynamics and anthropogenically forced changes in the Estanilles peat bog (southern
1271 Pyrenees) during the last seven millennia. Vegetation History and Archaeobotany 21,
1272 385-396.
1273
1274 Pérez-Sanz, A., González-Sampériz, P., Moreno, A., Valero-Garcés, B., Gil-Romera,
1275 G., Rieradevall, M., Tarrats, P., Lasheras-Álvarez, L., Morellón, M., Belmonte, A.,
1276 Sancho, C., Sevilla-Callejo, M., Navas, A., 2013. Holocene climate variability,
1277 vegetation dynamics and fire regime in the central Pyrenees: the Basa de la Mora
1278 sequence (NE Spain). Quaternary Science Reviews 73, 149-169.
1279
1280 Peyron, O., Goring, S., Dormoy, I., Kotthoff, U., Pross, J., Beaulieu, J.-L. de, Drescher-
1281 Schneider, R., Vannièrè, B., Magny, M., 2011. Holocene seasonality changes in the
1282 central Mediterranean region reconstructed from the pollen sequences of Lake Accesa
1283 (Italy) and Tenaghi Philippon (Greece). The Holocene 21, 131-146.
1284

1285 Pons, A., Reille, M., 1988. The holocene- and upper pleistocene pollen record from
1286 Padul (Granada, Spain): A new study. *Palaeogeography, Palaeoclimatology,*
1287 *Palaeoecology* 66, 243-263.
1288
1289 Pueyo, Y., Moret-Fernández, D., Saiz, H., Bueno, C.G., Alados, C.L., 2013.
1290 Relationships Between Plant Spatial Patterns, Water Infiltration Capacity, and Plant
1291 Community Composition in Semi-arid Mediterranean Ecosystems Along Stress
1292 Gradients. *Ecosystems* 16, 452-466.
1293
1294 Rasmussen, S.O., Vinther, B.M., Clausen, H.B., Andersen, K.K., 2007. Early Holocene
1295 climate oscillations recorded in three Greenland ice cores. *Quaternary Science Reviews*
1296 26, 1907-1914.
1297
1298 Reed, J.M., Stevenson, A.C., Juggins, S., 2001. A multi-proxy record of Holocene
1299 climatic change in southwestern Spain: the Laguna de Medina, Cádiz. *The Holocene* 11,
1300 707-719.
1301
1302 Reille, M., 1992. Pollen et Spores d'Europe et d'Afrique du Nord. Laboratoire de
1303 Botanique Historique et Palynologie. Marseille.
1304
1305 Reimer, P.J., Baillie, M., Bard, E., Bayliss, A., Beck, J.W., Blackwell, P.G., Bronk
1306 Ramsey, C., Buck, C.E., Burr, G., Edwards, R.L., 2009. IntCal09 and Marine09
1307 radiocarbon age calibration curves, 0-50,000 years cal BP. *Radiocarbon* 51, 1111-1150.
1308
1309 Renssen, H., Seppä, H., Heiri, O., Roche, D.M., Goosse, H., Fichefet, T., 2009. The
1310 spatial and temporal complexity of the Holocene thermal maximum. *Nature Geoscience*
1311 2, 411-414.
1312
1313 Rico, M.T., Sancho-Marcén, C., Arenas-Abad, M.C., Vázquez-Urbez, M., Valero-
1314 Garcés, B.L., 2013. El sistema de barreras tobáceas Holocenas de las Parras de Martín
1315 (Cordillera Ibérica, Teruel). *Cuadernos de Investigación Geográfica* 39, 141-158.
1316
1317 Rimbu, N., Lohmann, G., Kim, J.-H., Arz, H.W., Schneider, R., 2003. Arctic/North
1318 Atlantic Oscillation signature in Holocene sea surface temperature trends as obtained
1319 from alkenone data. *Geophysical Research Letters* 30, 1280.
1320
1321 Roca, J.R., Julià, R., 1997. Late-glacial and Holocene lacustrine evolution based on
1322 ostracode assemblages in Southeastern Spain. *Geobios* 30, 823-830.
1323
1324 Romero-Viana, L., Julià, R., Schimmel, M., Camacho, A., Vicente, E., Miracle, M.R.,
1325 2011. Reconstruction of annual winter rainfall since AD 1579 in central-eastern Spain
1326 based on calcite laminated sediment from Lake La Cruz. *Climatic change* 107, 343-361.
1327
1328 Rubiales, J.M., García-Amorena, I., García-Álvarez, S., Morla, C., 2009.
1329 Anthracological evidence suggests naturalness of *Pinus pinaster* in inland southwestern
1330 Iberia. *Plant Ecology* 200, 155-160.
1331
1332 Rubiales, J.M., García-Amorena, I., Hernández, L., Génova, M., Martínez, F.,
1333 Manzanque, F.G., Morla, C., 2010. Late Quaternary dynamics of pinewoods in the
1334 Iberian Mountains. *Review of Palaeobotany and Palynology* 162, 476-491.

1335
1336 Rubiales, J.M., Hernández, L., Romero, F., Sanz, C., 2011. The use of forest resources
1337 in central Iberia during the Late Iron Age. Insights from the wood charcoal analysis of
1338 Pintia, a Vaccaean oppidum. *Journal of Archaeological Science* 38, 1-10.
1339
1340 Rubio, J.C., 2004. Contexto hidrogeológico e histórico de los humedales del Cañizar.
1341 Consejo de la Protección de la Naturaleza de Aragón, Serie de Investigación, Zaragoza.
1342
1343 Sánchez Goñi, M.F., Hannon, G.E., 1999. High-altitude vegetational pattern on the
1344 Iberian Mountain Chain (north-central Spain) during the Holocene. *The Holocene* 9, 39-
1345 57.
1346
1347 Sancho, C., Peña, J.L., Meléndez, A., 1997. Controls on Holocene and present-day
1348 travertine formation in the Guadalaviar River (Iberian Chain, NE Spain). *Zeitschrift für*
1349 *Geomorphologie* 41, 289-307.
1350
1351 Sancho, C., Muñoz, A., González-Sampériz, P., Cinta Osácar, M., 2011.
1352 Palaeoenvironmental interpretation of Late Pleistocene–Holocene morphosedimentary
1353 record in the Valsalada saline wetlands (Central Ebro Basin, NE Spain). *Journal of Arid*
1354 *Environments* 75, 742-751.
1355
1356 Schnurrenberger, D., Russell, J., Kelts, K., 2003. Classification of lacustrine sediments
1357 based on sedimentary components. *Journal of Paleolimnology* 29, 141-154.
1358
1359 Sebastián López, S., 1989. Cella: historia y arte. *Revista Xiloca* 3, 91-96.
1360
1361 Simón-Gómez, J., 1989. Late Cenozoic stress field and fracturing in the Iberian Chain
1362 and Ebro Basin (Spain). *Journal of Structural Geology* 11, 285-294.
1363
1364 Shakun, J.D., Carlson, A.E., 2010. A global perspective on Last Glacial Maximum to
1365 Holocene climate change. *Quaternary Science Reviews* 29, 1801-1816.
1366
1367 Stevenson, A.C., 2000. The Holocene forest history of the Montes Universales, Teruel,
1368 Spain. *The Holocene* 10, 603-610.
1369
1370 Stuiver, M., Reimer, P.J., 1993. Extended (super 14) C data base and revised CALIB
1371 3.0 (super 14) C age calibration program. *Radiocarbon* 35, 215-230.
1372
1373 Stuiver, M., Grootes, P.M., Braziunas, T.F., 1995. The GISP2 $\delta^{18}O$ Climate Record of
1374 the Past 16,500 Years and the Role of the Sun, Ocean, and Volcanoes. *Quaternary*
1375 *Research*. 44, 341–354.
1376
1377 Tinner, W., Lotter, A.F., 2001. Central European vegetation response to abrupt climate
1378 change at 8.2 ka. *Geology* 29, 551-554.
1379
1380 Tinner, W., Kaltenrieder, P., 2005. Rapid responses of high-mountain vegetation to
1381 early Holocene environmental changes in the Swiss Alps. *Journal of Ecology* 93, 936-
1382 947.
1383

Con formato: Inglés (Estados Unidos)

Con formato: Inglés (Estados Unidos)

1384 Tzedakis, P.C., 2007. Seven ambiguities in the Mediterranean palaeoenvironmental
1385 narrative. *Quaternary Science Reviews* 26, 2042-2066.
1386

1387 Utrilla, P., Domingo, R., Montes, L., Mazo, C., Rodanés, J.M., Blasco, F., Alday, A.,
1388 2012. The Ebro Basin in NE Spain: A crossroads during the Magdalenian. *Quaternary*
1389 *International* 272-273, 88-104.
1390

1391 Valero-Garcés, B.L., Delgado-Huertas, A., Navas, A., Machín, J., González-Sampériz,
1392 P., Kelts, K., 2000a. Quaternary palaeohydrological evolution of a playa lake: Salada
1393 Mediana, central Ebro Basin, Spain. *Sedimentology* 47, 1135-1156.
1394

1395 Valero-Garcés, B.L., González-Sampériz, P., Delgado-Huertas, A., Navas, A., Machín,
1396 J., Kelts, K., 2000b. Lateglacial and Late Holocene environmental and vegetational
1397 change in Salada Mediana, central Ebro Basin, Spain. *Quaternary International* 73-74,
1398 29-46.
1399

1400 Valero-Garcés, B.L., González-Sampériz, P., Navas, A., Machín, J., Delgado-Huertas,
1401 A., Peña-Monné, J.L., Sancho-Marcén, C., Stevenson, T., Davis, B., 2004.
1402 Paleohydrological fluctuations and steppe vegetation during the last glacial maximum in
1403 the central Ebro valley (NE Spain). *Quaternary International* 122, 43-55.
1404

1405 Valero-Garcés, B.L., Moreno, A., Navas, A., Mata, P., Machín, J., Delgado Huertas, A.,
1406 González Sampériz, P., Schwalb, A., Morellón, M., Cheng, H., Edwards, R.L., 2008.
1407 The Taravilla lake and tufa deposits (Central Iberian Range, Spain) as
1408 palaeohydrological and palaeoclimatic indicators. *Palaeogeography, Palaeoclimatology,*
1409 *Palaeoecology* 259, 136-156.
1410

1411 van Geel, B., Buurman, J., Waterbolk, H.T., 1996. Archaeological and palaeoecological
1412 indications of an abrupt climate change in The Netherlands, and evidence for
1413 climatological teleconnections around 2650 BP. *Journal of Quaternary Science* 11, 451-
1414 460.
1415

1416 Vannièrè, B., Power, M.J., Roberts, N., Tinner, W., Carrión, J., Magny, M., Bartlein, P.,
1417 Colombaroli, D., Daniau, A.L., Finsinger, W., Gil-Romera, G., Kaltenrieder, P., Pini,
1418 R., Sadori, L., Turner, R., Valsecchi, V., Vescovi, E., 2011. Circum-Mediterranean fire
1419 activity and climate changes during the mid-Holocene environmental transition (8500-
1420 2500 cal. BP). *The Holocene* 21, 53-73.
1421

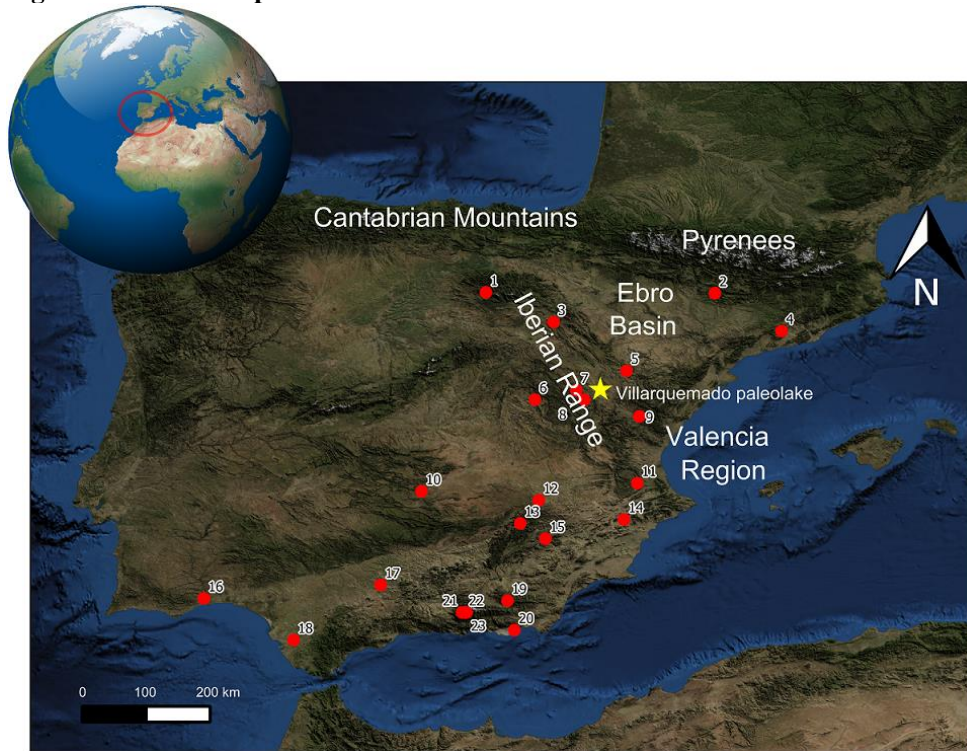
1422 Vegas, J., Ruiz-Zapata, B., Ortiz, J.E., Galán, L., Torres, T., García-Cortés, Á., Gil-
1423 García, M.J., Pérez-González, A., Gallardo-Millán, J.L., 2010. Identification of arid
1424 phases during the last 50 cal. ka BP from the Fuentillejo maar-lacustrine record (Campo
1425 de Calatrava Volcanic Field, Spain). *Journal of Quaternary Science* 25, 1051-1062.
1426

1427 Vegas-Vilarrúbia, T., González-Sampériz, P., Morellón, M., Gil-Romera, G., Pérez-
1428 Sanz, A., Valero-Garcés, B., in press. Diatom and vegetation responses to late glacial
1429 and Early-Holocene climate changes at Lake Estanya (Southern Pyrenees, NE Spain).
1430 *Palaeogeography, Palaeoclimatology, Palaeoecology* 392, 335-249.
1431

1432 Vicente-Redón, J.D., 2002. La presencia de Roma en la actual provincial de Teruel.
1433 Instituto de Estudios Turolenses, Teruel.

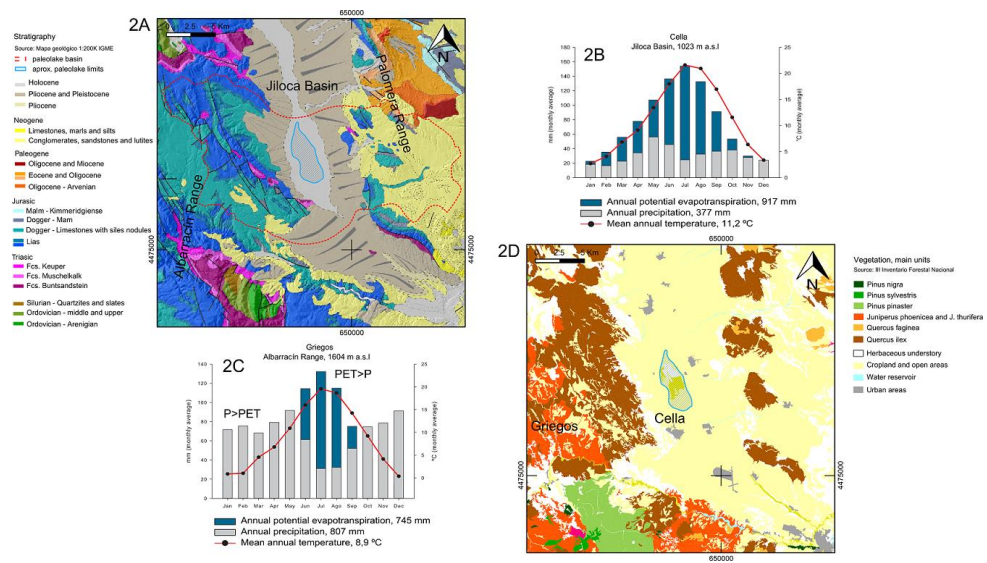
1434
 1435 Vicente-Serrano, S.M., Zouber, A., Lasanta, T., Pueyo, Y., 2012. Dryness is
 1436 accelerating degradation of vulnerable shrublands in semiarid Mediterranean
 1437 environments. *Ecological Monographs* 82, 407-428.
 1438
 1439 Wanner, H., Beer, J., Bütikofer, J., Crowley, T.J., Cubasch, U., Flückiger, J., Gossé,
 1440 H., Grosjean, M., Joos, F., Kaplan, J.O., Küttel, M., Müller, S.A., Prentice, I.C.,
 1441 Solomina, O., Stocker, T.F., Tarasov, P., Wagner, M., Widmann, M., 2008. Mid- to
 1442 Late Holocene climate change: an overview. *Quaternary Science Reviews* 27, 1791-
 1443 1828.
 1444
 1445 Zanchetta, G., Drysdale, R.N., Hellstrom, J.C., Fallick, A.E., Isola, I., Gagan, M.K.,
 1446 Pareschi, M.T., 2007. Enhanced rainfall in the Western Mediterranean during deposition
 1447 of sapropel S1: stalagmite evidence from Corchia cave (Central Italy). *Quaternary*
 1448 *Science Reviews* 26, 279-286.
 1449

1450 **Figures and tables caption**

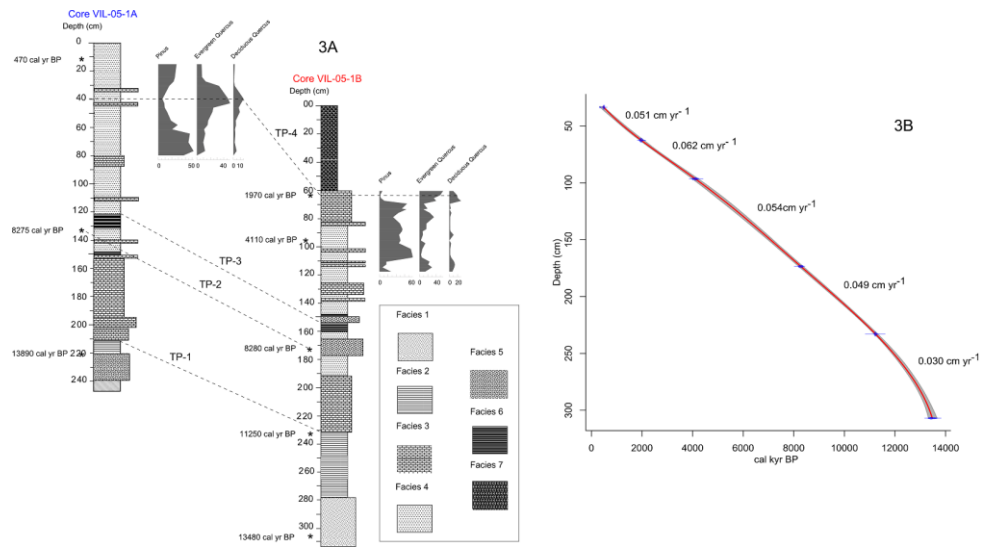


1451
 1452
 1453 **Figure 1.** Location of the Villarquemado paleolake in the Iberian Peninsula. The sites
 1454 cited in the discussion and in **Figures 7 and 8** are also included; 1) Las Pardillas Lake
 1455 (Sánchez-Goñi and Hannon, 1999); 2) Lake Estanya (Morellón et al., 2009; Vegas-
 1456 Vilarrúbia et al., 2013); 3) Añavieja River system (Luzón et al., 2011); 4) Cova de la

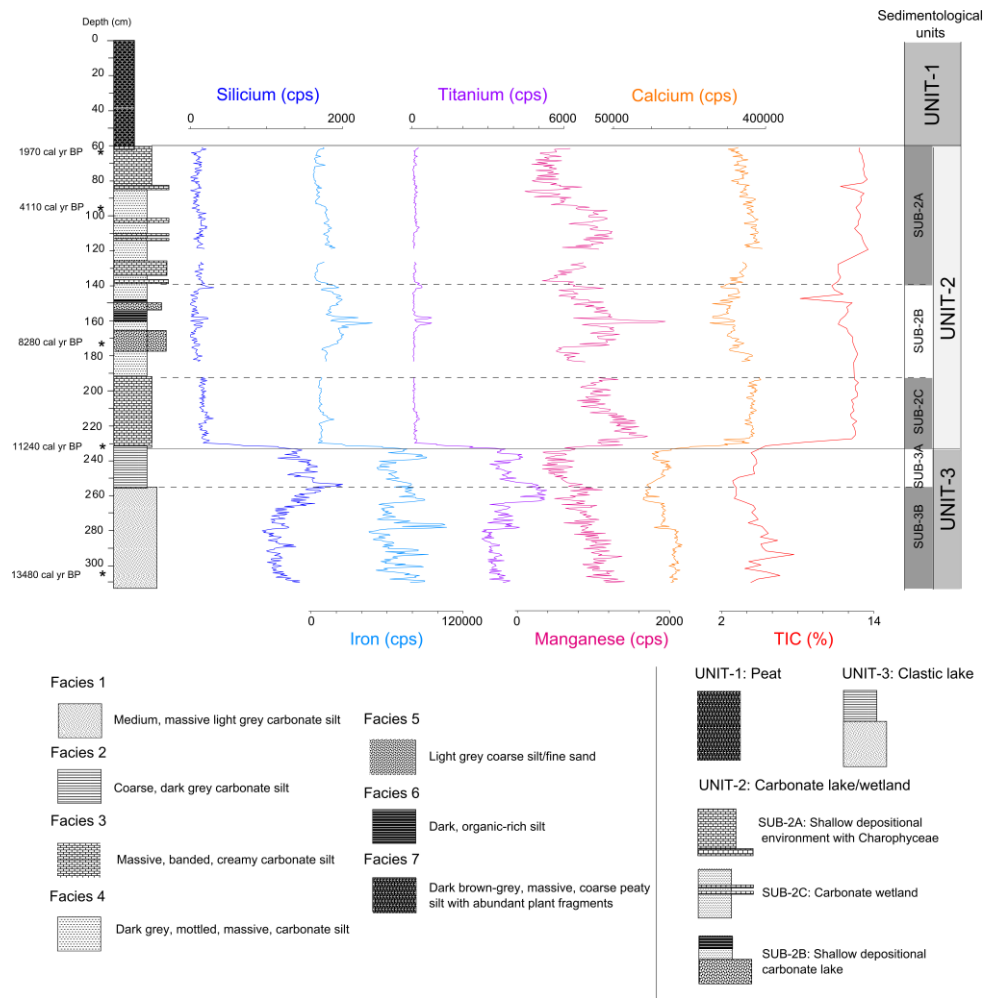
1457 Guineu (Allué et al., 2009); 5) Las Parras River system (Rico et al., 2013); 6) Trabaque
 1458 Canyon (Domínguez-Villar et al., 2012); 7) Ojos del Tremedal (Stevenson, 2000); 8)
 1459 Guadalaviar River system (Sáncho et al., 1997); 9) Mijares River system (Peña et al.,
 1460 2000); 10) Fuentillejo Maar (Vegas et al., 2010); 11) Navarrés (Carrión and van Geel,
 1461 1999); 12) Villaverde (Carrión et al., 2001); 13) Siles (Carrión, 2002); 14) Salines
 1462 (Roca and Julià, 1997); 15) El Sabinar (Carrión et al., 2004); 16) Guadiana Estuary,
 1463 Core CM5 (Fletcher et al., 2007); 17) Lake Zoñar (Martín-Puertas et al., 2008); 18)
 1464 Laguna de Medina (Reed et al., 2001); 19) Baza (Carrión et al., 2007); 20) San Rafael
 1465 (Pantaleón-Cano et al., 2003); 21) Laguna de la Mula (Jiménez-Moreno et al., 2013);
 1466 22) Borreguiles de la Virgen (Jiménez-Moreno and Anderson, 2012; García-Alix et al.,
 1467 2012); 23) Laguna del Río Seco (Andersón et al., 2011).



1468
 1469 **Figure 2.** (A) Main geological, (B and C) climatic and (D) vegetational features of the
 1470 Jiloca Basin.

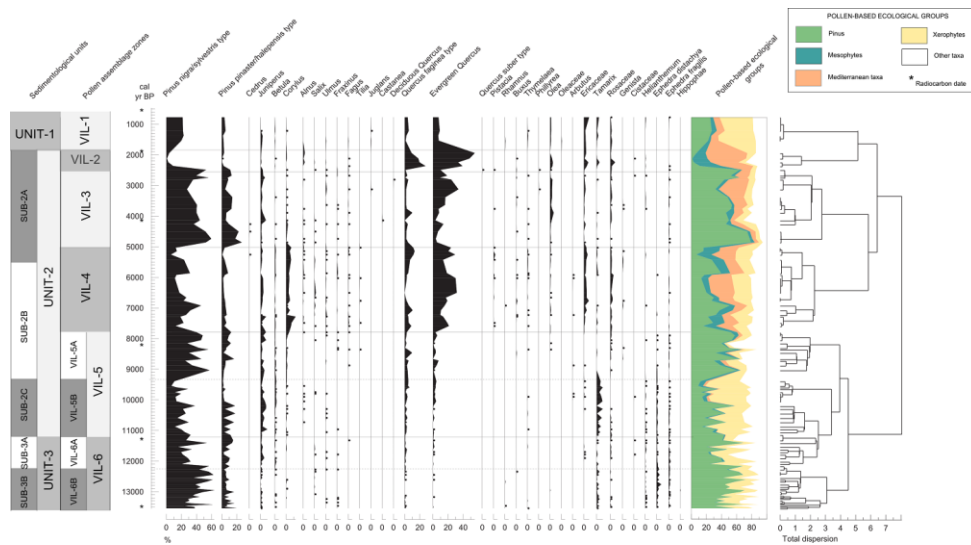


1471
 1472 **Figure 3.** (A) Correlation of VIL-05-1A and VIL-05-1B cores based on
 1473 sedimentological markers, ¹⁴C dates and main palynological changes. (B) Composite
 1474 depth-age model for the Villarquemado paleolake based on lineal interpolation of ¹⁴C
 1475 data (Table 1), obtained using the *Clam* software (Blaauw, 2010). The grey envelope
 1476 shows the 95% confidence interval.



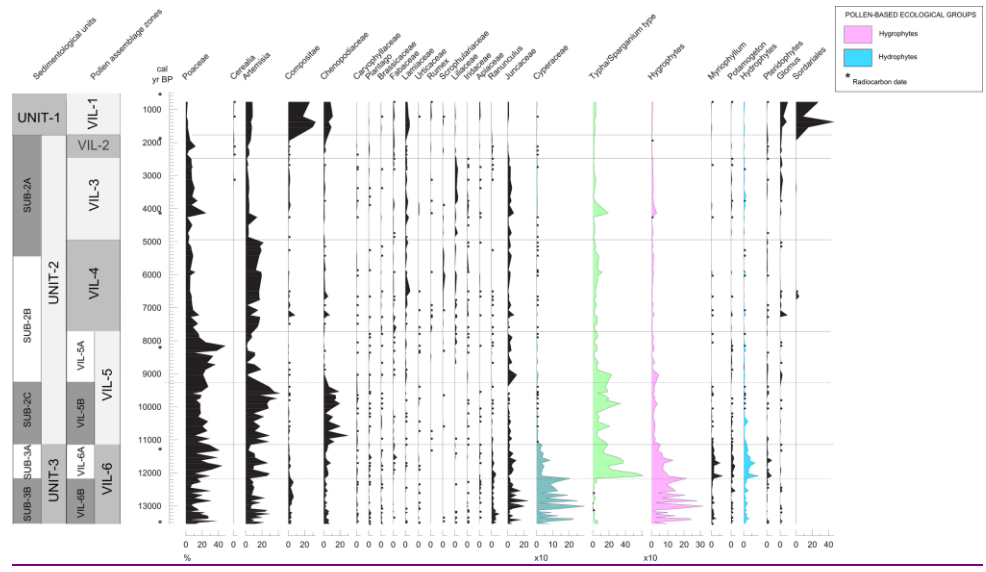
1477

1478 **Figure 4.** Sedimentary facies and sedimentological units, XRF analyses and TIC results
 1479 for the Villarquemado sequence. XRF intensities are expressed in counts per second
 1480 (cps) and TIC values in percentages. The facies description is supported by X-ray
 1481 diffraction and visual inspection of relative mineral abundances on smear slides.



1482

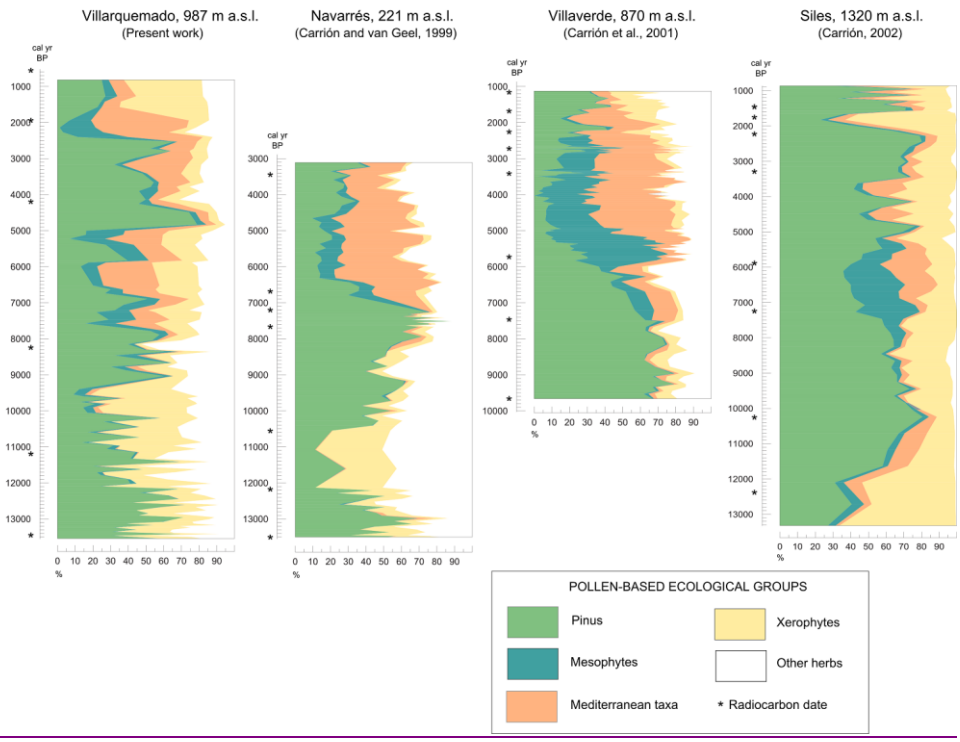
1483 **Figure 5.** Pollen diagram from Villarquemado sequence for trees and shrubs.
 1484 Mesophytes-group comprises *Betula*, *Corylus*, *Alnus*, *Salix*, *Ulmus*, *Fraxinus*, *Fagus*,
 1485 *Tilia*, *Juglans*, *Castanea*, deciduous *Quercus* and *Quercus faginea* type; Mediterranean
 1486 taxa-group is composed by Evergreen *Quercus*, *Quercus suber* type, *Pistacia*, *Rhamnus*,
 1487 *Buxus*, *Thymelaea*, *Phillyrea*, *Olea*, Oleaceae and *Arbutus*; Xerophytes-group is formed
 1488 by *Juniperus*, *Helianthemum*, *Ephedra distachya*, *E. fragilis*, *Hippophae*, *Artemisia*,
 1489 Compositae and Chenopodiaceae; Other herbs-group includes Rubiaceae, *Gentiana*,
 1490 Boraginaceae, Plumbaginaceae, *Armeria*, Primulaceae, *Papaver*, Geraniaceae,
 1491 Malvaceae, Violaceae, Polygonaceae, *Crocus*, *Cytisus*, *Asphodelus*, *Galium*,
 1492 Valerianaceae, Dipsacaceae, *Aristolochia* and *Cannabis/Humulus* type. Dots represent
 1493 percentages <0.5%. Sedimentological units defined in Figure 4 are also reported to
 1494 facilitate readability.



1495

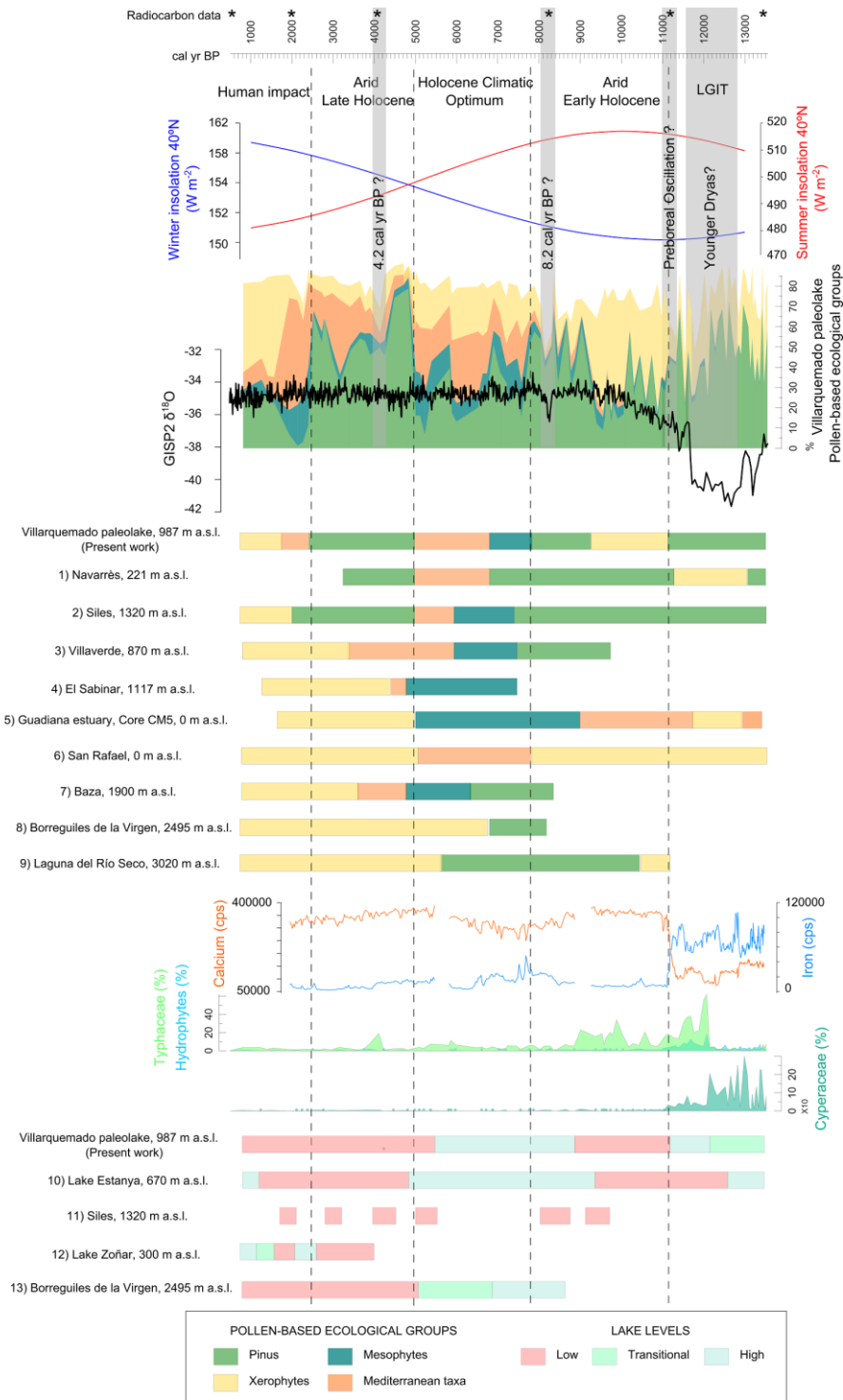
1496 **Figure 6.** Pollen diagram from Villarquemado sequence for herbs, hygrophytes,
 1497 hydrophytes, Pteridophytes and NPPs. Hygrophytes-group is composed by *Ranunculus*,
 1498 Juncaceae, Cyperaceae, *Typha/Sparganium* type and *Thalictrum*. Hydrophytes-group
 1499 includes *Myriophyllum*, *Potamogeton*, *Utricularia*, *Nuphar*, *Nymphaea* and *Callitriche*.
 1500 Dots represent percentages <0.5%. Sedimentological units defined in Figure 4 are also
 1501 reported to facilitate

1502 readability.



1503

1504 **Figure 7.** Main vegetation trends in the Villarquemado sequence and correlation with
1505 other Mediterranean continental records. Pollen-based ecological groups for
1506 Villarquemado are defined in [Figure 5](#) caption. Pollen data for Navarrés, Villaverde and
1507 Siles have been obtained from [Carrión and van Geel \(1999\)](#), [Carrión et al. \(2001\)](#) and
1508 [Carrión \(2002\)](#), respectively.



1509

1510 **Figure 8.** Comparison of the Villarquemado sequence (pollen-based ecological groups,
 1511 top; aquatic taxa and geochemical composition, center) with selected records from

1512 continental Iberia for the Lateglacial and Holocene derived from various approaches.
 1513 Winter and summer insolation values for 40°N are calculated by means of PAST
 1514 software (Hammer et al., 2001) and GISP2 isotope values obtained from Stuiver et al.,
 1515 (1995). Pollen data have been acquired from 1) Navarrés (Carrión and van Geel, 1999);
 1516 2) Siles (Carrión, 2002); 3) Villaverde (Carrión et al., 2001); 4) El Sabinar (Carrión et
 1517 al., 2004); 5) Core CM5 (Fletcher et al., 2007); 6) San Rafael (Pantaleón-Cano et al.,
 1518 2003); 7) Baza (Carrión et al., 2007); 8) Borreguiles de la Virgen (Jiménez-Moreno and
 1519 Anderson, 2012) and 9) Laguna del Río Seco (Anderson et al., 2011). The main lake
 1520 level phases are derived from 10) Lake Estanya (Morellón et al., 2009); 11) Siles
 1521 (Carrión, 2002); 12) Lake Zoñar (Martín-Puertas et al., 2008); and 13) Borreguiles de la
 1522 Virgen (García-Alix et al., 2012). Pollen-based ecological groups for Villarquemado
 1523 defined in the caption of Figures 5 and 6 and lake level reconstructions have been
 1524 summarized by integrating sedimentological, geochemical and hygro-hydrophyte pollen
 1525 assemblages.

1526 **Table 1.** Radiocarbon dates (AMS) for the Villarquemado sequence obtained from bulk
 1527 sediment.

<u>Core</u>	<u>Lab. number</u>	<u>Depth (cm)</u>	<u>Radiocarbon date</u> <u>(¹⁴C AMS yr BP)</u>	<u>Age error</u> <u>(yr BP)</u>	<u>Calibrated age (2σ)</u> <u>(cal. yr BP)</u>
<u>VIL-05-1A</u>	<u>Beta-332033</u>	<u>11</u>	<u>430</u>	<u>30</u>	<u>529-431</u>
<u>VIL-05-1A</u>	<u>Beta-332034</u>	<u>132</u>	<u>7460</u>	<u>40</u>	<u>8365-8190</u>
<u>VIL-05-1A</u>	<u>Poz-16073</u>	<u>220</u>	<u>11950</u>	<u>70</u>	<u>13997-13617</u>
<u>VIL-05-1B</u>	<u>Beta-319544</u>	<u>62.5</u>	<u>2020</u>	<u>30</u>	<u>2084-1898</u>
<u>VIL-05-1B</u>	<u>Poz-18451</u>	<u>96.5</u>	<u>3750</u>	<u>40</u>	<u>4232-3990</u>
<u>VIL-05-1B</u>	<u>Poz-18509</u>	<u>173.5</u>	<u>7460</u>	<u>50</u>	<u>8373-8185</u>
<u>VIL-05-1B</u>	<u>Poz-18453</u>	<u>233</u>	<u>9820</u>	<u>50</u>	<u>11339-11192</u>
<u>VIL-05-1B</u>	<u>Poz-15943</u>	<u>307</u>	<u>11620</u>	<u>60</u>	<u>13645-13306</u>

1529

1530

1531